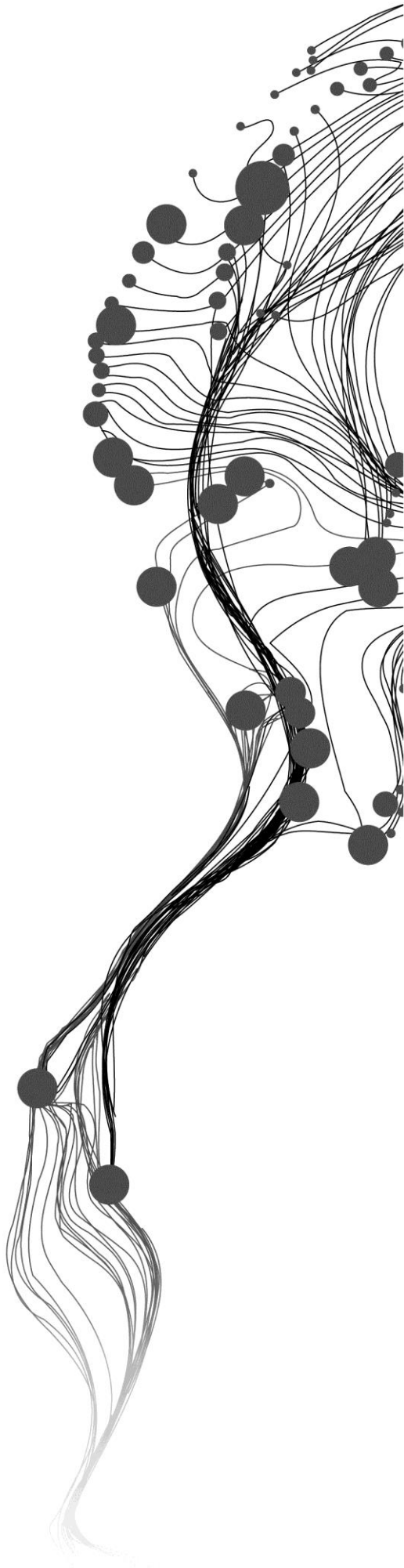


ANALYSIS OF BUILDING OUTLINE QUALITY BY COMPARISON TO DENSE POINT CLOUDS

IDU EMMANUEL Y.
March, 2015

SUPERVISORS:
Prof. Dr. Ir. M. G. Vosselman
Dr. K. Khoshelham



ANALYSIS OF BUILDING OUTLINE QUALITY BY COMPARISON TO DENSE POINT CLOUDS

IDU EMMANUEL Y.

Enschede, The Netherlands, March, 2015

Thesis submitted to the Faculty of Geo-Information Science and Earth Observation of the University of Twente in partial fulfilment of the requirements for the degree of Master of Science in Geo-information Science and Earth Observation.
Specialization: Geoinformatics.

SUPERVISORS:

Prof. Dr. Ir. M. G. Vosselman

Dr. K. Khoshelham

THESIS ASSESSMENT BOARD:

Prof. Dr. Ir. A. Stein (Chair)

Dr. R. C. Lindenberg (External Examiner, Delft University of Technology)

DISCLAIMER

This document describes work undertaken as part of a programme of study at the Faculty of Geo-Information Science and Earth Observation of the University of Twente. All views and opinions expressed therein remain the sole responsibility of the author, and do not necessarily represent those of the Faculty.

ABSTRACT

Following the request from the Municipal of Rotterdam to determine the quality of the 2D maps in their registry using the newly acquired ALS data, this thesis focuses on determining measures that will be used to identify, separate, measure and classify differences on the map by comparing with point cloud data from an Airborne Laser Scanning system. This approach is vector based which first applies a symmetrical difference operation to identify differences between outlines from the 2D map and outlines derived from point clouds. These differences are separated into two sets using a threshold value; the two sets are the large and small differences. The small differences are used to determine the geometric accuracy of the map by statistically analysing point-to-line distance measurements. The accuracy of the map is reported to be approximately 25cm. The large differences are further classified into four classes – sunshades, building extensions, vegetation and mixed objects – by employing a supervised classification scheme on the height distribution of the laser point clouds. A 70% overall accuracy is derived for this classification.

ACKNOWLEDGEMENTS

To my ever supportive and inspiring supervisor, Prof. Dr. Ir. M. G. Vosselman; my cool second supervisor, Dr. K. Khoshelham; my fellow laser colleagues and special pals, Josyline and Bernard; my unforgettable GFM clique; my programming advisers Claudio, Luiz and Alfredo; my loving parents and siblings; my precious Enya; my bosses and mentors, Survs. Uche and Ibe; my Surveyor-General, Surv. Oku; my great colleagues Survs. Ibi, Timothy and Magnus; Kalita, Leo, Emmarasak, Efiom, Egbon and Cyrus; Majaja and family; my cherished Dr. Ugo and family; and my invisible but invincible sponsors, Nuffic – I thank you all.

As I grow older and wiser, I will always look back to this period when you all made my days memorable with your overwhelming support and encouragement. Grazie.

.

TABLE OF CONTENTS

1.	INTRODUCTION	1
1.1.	Motivation and problem statement	1
1.2.	Research identification	2
1.2.1.	Research objectives	2
1.2.2.	Research questions	2
1.2.3.	Innovation	3
1.3.	Structure of the thesis	3
2.	LITERATURE REVIEW	5
2.1.	Introduction to change detection	5
2.2.	Change detection with airborne laser scanning data	6
2.3.	Working with 2D maps	10
2.4.	Quality of LiDAR data	11
2.5.	Quality assessments in change detection	12
3.	PROCESS IMPLEMENTATION	14
3.1.	Data	16
3.2.	Data Preparation	17
3.2.1.	The point clouds	17
3.2.2.	The map data	19
3.3.	Building outlines from point cloud	20
3.4.	Overlay Analysis	21
3.5.	Distinguishing the kinds of changes	22
4.	DETERMINATION OF GEOMETRIC ACCURACY OF THE 2D MAP	24
4.1.	Finding the Geometric Accuracy of the map	24
4.1.1.	The uncertainty in outlining because of the point spacing	24
4.1.2.	The uncertainty in point location	25
4.1.3.	Finding the differences	25
4.1.4.	Assessment of the accuracy determination method	26
4.2.	Discussions of results for the geometric accuracy of map	26
5.	INTERPRETING LARGE DIFFERENCES	28
5.1.	Training Samples	28
5.2.	Statistical measures	30
5.3.	Formulating classification rules	33
5.4.	Accuracy assessment of classification	39
6.	CONCLUSION AND RECOMMENDATIONS	43
6.1.	Conclusion	43
6.2.	Recommendations	43

LIST OF FIGURES

Figure 2-1: Classification concept of change detection algorithms (Gong et al. 2008).	5
Figure 2-2: A difference image derived from subtracting two ALS data and a morphologically transformed image of the same scene after commission errors are removed. Culled from Murakami et al., (1999).	7
Figure 2-3: Change classification by Choi et al. (2009).	8
Figure 2-4: Change categories by Teo & Shih (2013).	9
Figure 2-5: Classification thresholds for change detection by Teo & Shih (2013).	9
Figure 2-6: Check for intrusion of laser segment by using the dilated laser segment and fitting to the generalised database object; for protrusion by using the eroded laser segment and fitting inside a generalised database object. Source: Vosselman et al., (2004).	10
Figure 2-7: Systematic offsets that may exist between building segments in a laser dataset and a vector map. Source: Vosselman et al., (2004).	11
Figure 2-8: Segments falsely marked as new buildings which were in fact omitted in the map due to mapping rules. Source: Vosselman et al., (2004).	11
Figure 2-9: offsets between identical ridgelines in an overlapping strip. Vosselman (2008).	12
Figure 3-1: Flow of processes in analysing change	15
Figure 3-2: Classified point clouds covering the study area	16
Figure 3-3: 2D map of the study area clipped from the Dutch registry BAG.	16
Figure 3-4: Tile-wise results after growing building segments.	17
Figure 3-5: Result of block segments operation executed after the grow segments function	18
Figure 3-6: Block segments result of study area.	18
Figure 3-7: Polygons before and after aggregation.	19
Figure 3-8: An example of Delaunay triangulation of a set of random points. (Source: Wikipedia, 2014) ..	20
Figure 3-9: over perforation of polygons caused by small clustering threshold and over generalisation due to large clustering threshold	20
Figure 3-10: Point clouds segment for a part of the block and the resulting outline for a building polygon	21
Figure 3-11: showing the differences in polygon datasets using symmetrical difference overlay analysis.	22
Figure 3-12: Use of bounding boxes with threshold values to distinguish points with large differences from points with small differences.	22
Figure 4-1: Sample of the effect of point distribution on the outline of an object and the line turned through every five degrees resulting in 72 lines	25
Figure 4-2: A clip of the study area showing the small differences.	26
Figure 5-1: Histogram of height distribution for a typical building extension.	29
Figure 5-2: Histogram of height distribution for a typical sunshade/balcony.	29
Figure 5-3: Histogram of height distribution for a typical vegetation class.	30
Figure 5-4: Scatter plot showing the number of significant bins against entropy values for the samples.	34
Figure 5-5: Scatter plot showing the number of significant bins against ground ratio for the samples.	34
Figure 5-6: Scatter plot showing the number of significant bins against number of points in samples.	34
Figure 5-7: Supposed sunshade with a clear roof and wall outline inside it.	35
Figure 5-8: Dense tree crown causing sparse distribution of ground points below it leaving gaps.	35
Figure 5-9: Classification algorithm for change polygons	37
Figure 5-10: Classification results overlaid on map outline.	38
Figure 5-11: A typical scenario where there is uncertainty in sunshade/building extension classification.	39

Figure 5-12: A likely “mixed object” class classified as building extension because of the overwhelming presence of building extension characteristics. 40

Figure 5-13: A supposed sunshade classified as vegetation because of the presence of overhanging trees. 40

Figure 5-14: Building polygons earmarked for updating and those that are unchanged. 42

Figure 6-1: Example of a deviation map showing spread of error magnitude. Source: Anil et al. (2013). .. 44

LIST OF TABLES

Table 4-1 Results for map accuracy calculated independently for 4 blocks.	26
Table 5-1: Number of significant bins for 5 samples in each class.	31
Table 5-2: Entropy values for 5 samples in each class.	32
Table 5-3: Ground ratio values derived for 5 samples in each class	33
Table 5-4: Rules used to define classes inferred from samples.	36
Table 5-5: Error matrix for assessing accuracy of the classification.	39

1. INTRODUCTION

1.1. Motivation and problem statement

The topic of change detection continuously sparks interests in the field of remote sensing. Its applications cut across various environmental fields. According to Singh (1989), change detection has been applied in “land use change analysis, monitoring of shifting cultivation, assessment of deforestation, study of changes in vegetation phenology, seasonal changes in pasture production, damage assessment, crop stress detection, disaster monitoring snow-melt measurements, day/night analysis of thermal characteristics and other environmental changes”. Nowadays, sensors with varying capabilities are developed frequently providing more possibilities in application fields but this also brings challenges on how the data obtained from them can be effectively used for specific applications like change detection.

In recent times, LiDAR (Light Detection and Ranging) has gained prominence in remote sensing, and has been used also for monitoring environmental events and detecting changes.

Change detection is usually executed to update maps and spatial databases by comparing datasets of two or more epochs. With LiDAR data, this can be done by comparing multi-temporal data like in (Murakami et al., 1999), (Teo and Shih, 2013), (Xu et al., 2013) and (Rutzinger et al., 2010) or by comparing a single epoch data with a particular map (Vosselman et al, 2004). Other media of comparisons may exist like when compared/combined with satellite images (Malpica et al., 2013).

In comparing maps, questions about their correspondence are often raised, these questions concern their spatial accuracy, the errors that may exist in each map, and the errors that may arise from the methods used to compare them. This calls for the need to evaluate and classify the kind of changes on the maps and further investigate the errors contained therein.

When change detection methods are implemented, general quality assessments are usually carried out to evaluate their performances and products obtained. Some common quantitative measures used are confusion matrix, completeness and correctness analyses (Freire et al., 2014). These measures are usually not sufficient for checking the quality of individual objects in terms of their spatial correlation or deviation from reference data of higher accuracy. Hence there is a shortcoming in analysing the geometric quality of specific objects derived from the methods applied.

Furthermore, in analysing quality issues, Vosselman et al. (2004) stressed on the importance of considering the rules and specifications employed when 2D maps are to be updated. One striking point was that change detection can be useful in identifying quality issues on 2D maps. If after change detection is implemented it is observed that some objects still contain errors, misalignments and displacements, then it becomes imperative that the reasons for such deviations are carefully investigated. Quality assessment/error analysis is applied if the differences are small and change classification if the differences are large.

Freire et al. (2014) have indicated that assessing quality of spatial information can be done by measuring its compliance with independent sources. Usually the quality of checking the accuracy of a certain map may involve the use of ground truth data from field surveys, but the challenge here is that such data is expensive and not sufficient to cover large areas. Another alternative is comparing with another dataset with larger accuracy; this is the approach to be adopted in this research in order to analyse the outline quality of buildings in a 2D map. Laser data proves to be an effective independent source of reference. There have been reported accuracies of 15-25cm planimetry (Rentsch and Krzystek, 2009) and subsequently this makes them suitable for updating and checking the quality of 2D maps.

Before LiDAR data can be used as quality control for a map, it is important to ascertain that it is fit for such purpose by assessing its internal quality (Oude Elberink and Vosselman, 2011). The specifications of the data are also critical in obtaining reliable information on the accuracies of the data.

With these numerous challenges, the motivation for this work lies in the need to employ measures for determining the accuracy of a base map by comparing with point cloud data of higher planimetric accuracy. The differences between the map and LiDAR data can be large, indicating a change, or small, indicating error in the map.

1.2. Research identification

1.2.1. Research objectives

The main objective of this research is to develop an improved procedure for checking the quality of a 2D base map by comparing changes with a LiDAR data set. This involves the following sub-objectives:

- a) To develop appropriate measures to assess the quality of a map.
- b) To separate the differences caused by real changes from the differences caused by errors in the map.
- c) To interpret the real changes caused by large differences in order to understand which changes are relevant and should lead to map updating.

1.2.2. Research questions

- 1) What suitable measures can be used to evaluate discrepancies between objects from 2D map and point cloud data?
- 2) How are differences caused by change and those caused by data inaccuracies discriminated?
- 3) Which features are suitable for change classification?
- 4) Which kind of changes can be distinguished?

1.2.3. Innovation

Innovatively, this study aims to:

- a) Implement change detection as a means to carrying out quality assessments on 2D maps.
- b) Derive classes for change based on error magnitude and error distribution.

This provides a new dimension to the application of change detection with emphasis on determination of geometric accuracy.

1.3. Structure of the thesis

This thesis is structured into six chapters. Chapter 1 contains the motivation and problem statement, the research objectives and questions, and the innovation. Chapter 2 reviews literature of closely related works on the topic. Chapter 3 introduces the processes employed with focus on the preparation of data. In chapter 4, a detailed analysis of the geometric accuracy determination is presented, the results are discussed too. Chapter 5 focuses on the interpretation of “large” changes. Chapter 6 is for the conclusion and recommendations from the author.

2. LITERATURE REVIEW

2.1. Introduction to change detection

The terms “monitoring” and “dynamic” are typically associated with change detection. Knowing that one constant factor in man’s environment is change; it comes as no surprise that scientist, especially in the field of environmental sciences, remote sensing and GIS, dedicate vast mental and financial resources in investigating the dynamics of landforms, objects and even people by employing critical monitoring and observation techniques. Change detection is therefore not a new thing to researchers. In the field of remote sensing, several sensors and methods have been employed, Gong et al., (2008) provide detailed descriptions of such techniques and methods by categorising the algorithms used in change detection as summarised in figure 2-1 below.

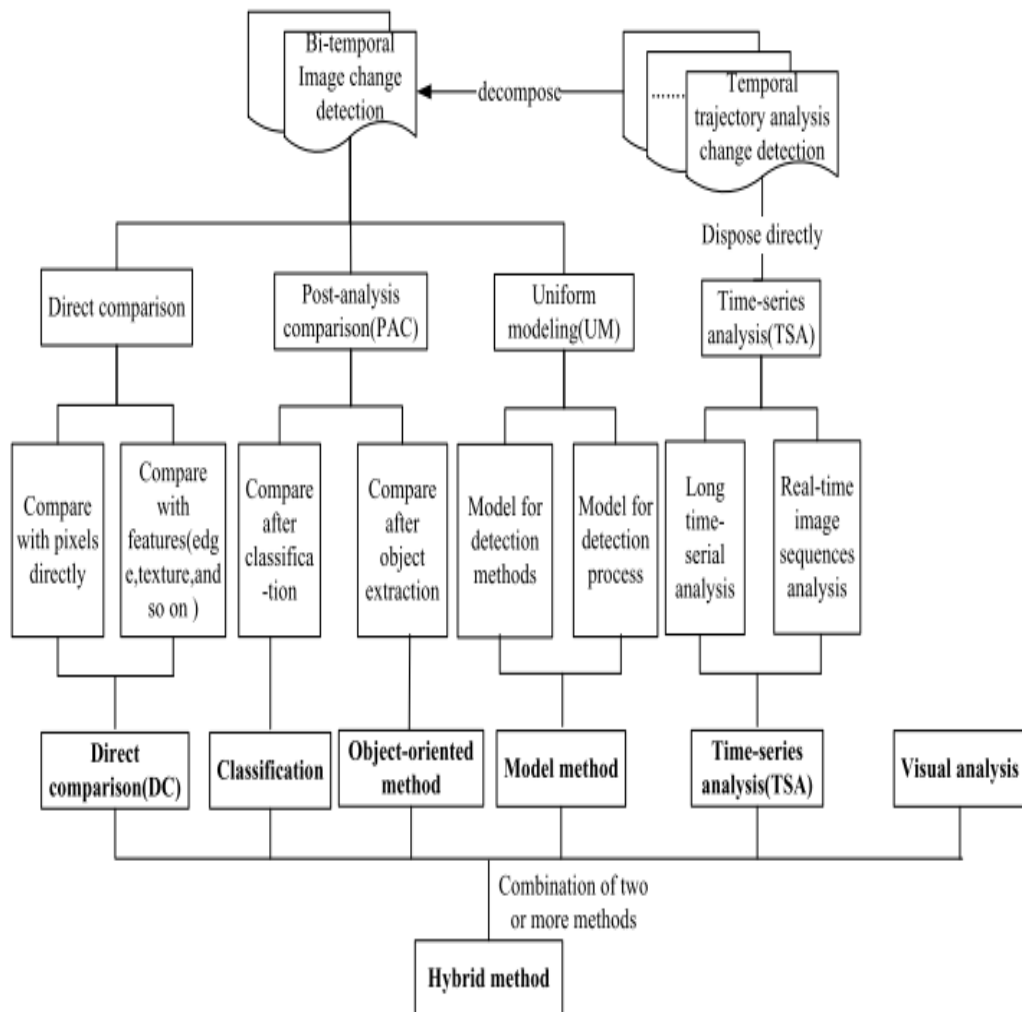


Figure 2-1: Classification concept of change detection algorithms (Gong et al. 2008).

In this description, change detection algorithms are grouped into seven classes – “direct comparison, classification, object-oriented method, time-series analysis, visual analysis and hybrid method”. The hybrid method usually consists of a combination of two or more of the other methods. The paper also talked on the effect and methods of geometric correction as well as the effect of radiometric correction. Geometric corrections were discussed to be prerequisites for the implementation of change detection algorithms as multi temporal images require a desirable level of spatial co-registration to minimise false indications of changes. It stressed that a sub-pixel level is accepted for geometric registration accuracy. However, there were instances where the reliability of the sub-pixel accuracies were questioned especially when different data sources are considered. In using multi-sensor images, several challenges are posed that affect the quality of geometric registration. These challenges are due to varying characteristics of the images such as “imaging models, imaging angles and conditions, curvature and rotation of the earth” etc. and are pronounced in areas of high terrain variability like in mountainous and urban scenes. The use of feature based methods of change detections are considered to be less demanding for registration accuracies since changes are detected on extracted objects, but the level of reliability of the results from such procedure are still yet to be fully investigated. On the issue of radiometric correction, the need to correct for external physical and environmental factors which often introduce what may be considered as noise on the images was also discussed, these kind of factors like cloud cover, different illumination angles etc. often affect change detection results and need to be corrected before changes are analysed. One aspect of correction which is termed absolute radiometric correction involves adjusting radiation values to standard values by manipulating spectral curves in the lab, this approach often comes with a great setback in reality because of the difficulty and cost in acquiring atmospheric parameters and ground objects (used as reference data) for current and past scenes. On the other hand, the relative radiometric correction is often used, as the characteristics of a reference image are used to correct the affected image; this is mostly done using histogram regularisation algorithms. This process however was adjudged to be unnecessary for feature based algorithms.

The application of any of the methods of change classification algorithms follows the pre-processing stage of radiometric and geometric corrections. Choosing which method to adopt often depends on the availability of resources, operator’s knowledge and competence, data sources, scene characteristics and a host of other factors. Each class possesses its own sets of merits and demerits and the choice of method depends on the analyst’s interpretation of the underlying circumstances. Consequently, assessments are implemented to ensure that the methods selected and used meet certain quality standards. These assessments are often based on the use of reference data which may be acquired with various approaches. Whatever approach is used, whether field survey, use of high resolution images or visual interpretations, it is worth mentioning that there are usually advantages and disadvantages which are dependent on the desired application and cost implications. The use of pixel based assessment have been prominent which leads to Gong et al., (2008) suggesting that more should be done to improve on object or feature based accuracy assessment methods.

2.2. Change detection with airborne laser scanning data

Already, a lot of research has been done on change detection using LiDAR data. Due to the limitations (which include time consuming processes, costly operations and inclusion of omission errors) of using the manual methods, Murakami et al., (1999) first employed the use of Airborne laser Scanning (ALS) data for detecting changes in buildings in the city of Minokama, Japan. The authors started by investigating the capabilities of the ALS data in meeting the requirements for detecting changes in an urban area where buildings could change in both vertical and horizontal dimensions. The initial consideration addressed objects on the scene which were considered to be a minimum of 2m by 2m in horizontal direction and

about 2m for minimum floor height; hence the expectation for the ALS was that it would be better than 1 meter in both directions for the changes to be effectively detected. An accuracy validation was done to conclude that the ALS data had a vertical accuracy of 10-20 cm and a horizontal accuracy of about 1m which made it suitable for the study. The approach simply employed differencing of multi-temporal digital surface models (DSM) to detect changes. To minimise commission errors, morphological operations were used to remove edges on objects that were unchanged. The selected threshold for the operation was based on the value derived for the horizontal accuracy of the ALS data. The authors argued that by eliminating the omission errors, manual inspection will be focused on areas with actual changes which in turn will address the removal of commission errors in a more simplistic manner thereby saving time.

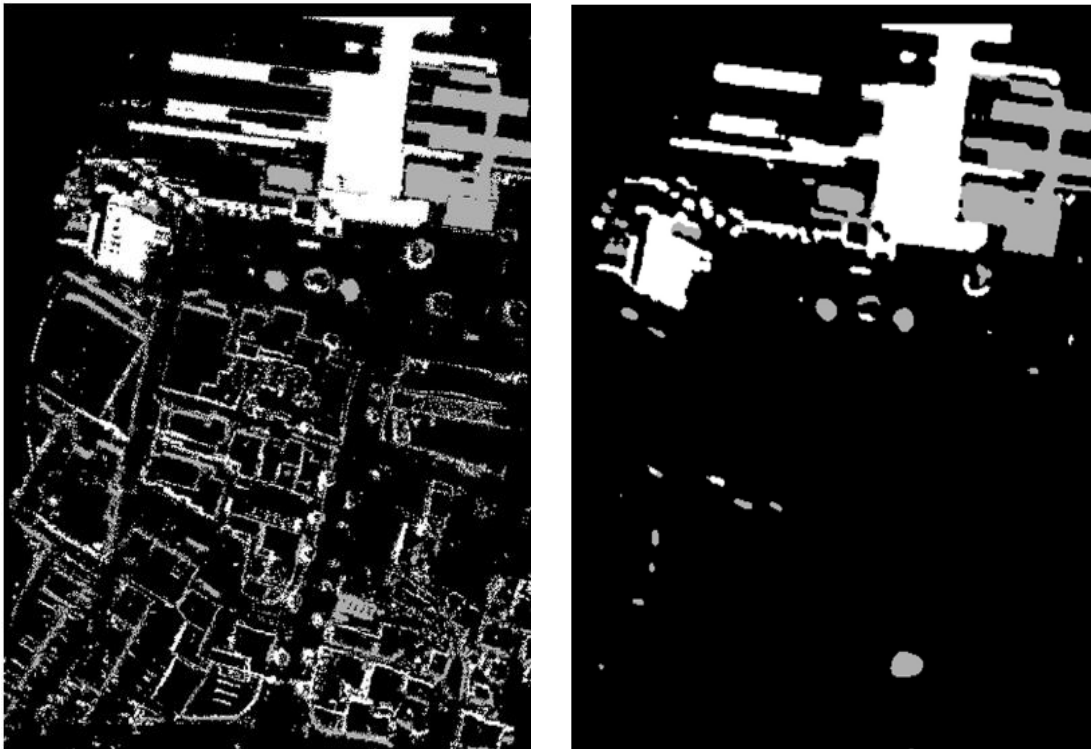


Figure 2-2: A difference image derived from subtracting two ALS data (left) and a morphologically transformed image of the same scene after commission errors are removed (right). Culled from Murakami et al., (1999).

Since achieving this feat which was automatic, LiDAR based change detection has taken several approaches and automation remains the main goal for some of the methods adopted. Matikainen et al., (2010) used DSM derived from airborne laser scanner data in combination with digital aerial image to initiate the change detection process and later applied object based image analysis on individual building objects to update base maps. The approach used three sets of data; ALS data, colour ortho image mosaic and two building maps. All data were processed in raster formats. The ALS data was classified into ground and non-ground where points above the threshold of 2.5m were considered to be non-ground. The ortho mosaic was generated using DSM derived from the ALS data and images from an aerial digital camera. The map data was fetched from an existing database and the most recent one was adjusted to create an old map by removing new buildings and adding demolished ones. To start the comparison, buildings were first detected in the ALS data by implementing a segmentation algorithm which first separated buildings and trees from the ground surface. A further classification was adopted which used decision tree methods based on training sets to split the trees from the buildings. The decision tree produced two sets of

building-tree classes for low rise area and other areas. The resultant building objects (derived with an accuracy of 89%) were used for change detection by comparing with the existing building map. The change detection method (object based) compared and matched map objects by using overlap analysis and buffers from morphological operations. This resulted in five classes for the building change objects, the classes are unchanged, changed, new, demolished and 1-n/n-1 buildings (this class refers to buildings changes that may accrue from map generalisation, inaccuracy of the map or problems with detecting buildings). The assessment of this method showed that there was 80% and 77% completeness and correctness respectively in detecting buildings larger than 20m².

Choi et al. (2009) presented a feature based approach to classify changes from multi-temporal Airborne Laser Scanning (ALS) data. Points were grouped into patches after subtracting DSMs of different epochs like in the case of Murakami et al. (1999). A difference image derived by this differencing is similarly corrected for commission errors by using opening operation. To further improve on the classification of the changes, clues of changes are derived from the point cloud data which undergoes a segmentation process. The segments referred to as surface patches are then grouped into clusters based on their connectedness (which simply considers horizontal characteristics of the changes) and elevatedness (which models the proportional changes in height). The first classification of the surface patches yields three classes of ground, vegetation and building. This was achieved by considering the roughness, size and height of the patches derived. Having achieved this with the separate DSMs, the patches from each DSM are compared on a grid basis using the height, roughness and normal vectors of the patches. With these properties, the changes in classes are grouped into ten categories.

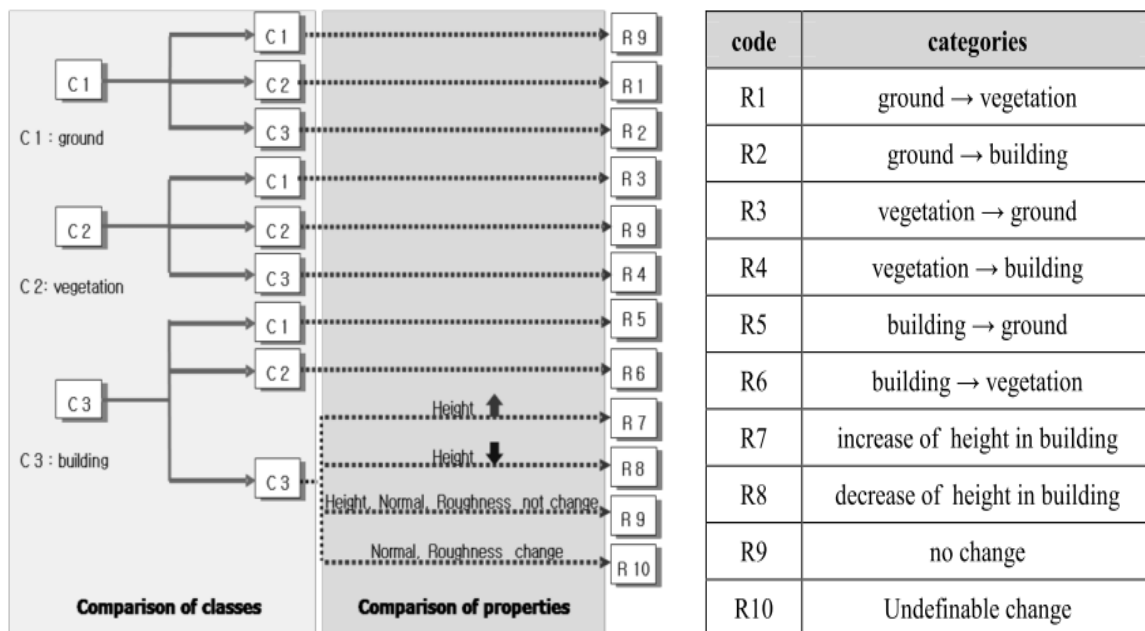


Figure 2-3: Change classification by Choi et al. (2009) derived from three major classes of patches(left) and the resultant categories from analysing the height, roughness and normal vector of corresponding patches (right).

The results were reported to be satisfactory when compared with an orthoimage background, though no quantitative analysis was carried for the exercise.

Similarly, Teo and Shih (2013) generated shape difference map from two DSMs of different epochs. Areas with small differences were considered as unchanged areas and the large differences were subjected to segmentation and classification. The procedure started with the usual pre-processing methods of co-registration followed by the already familiar differencing of DSMs. Segmentation was also implemented before the classification of changes was computed. The classification focused on buildings and vegetation. In this case the gradient magnitude was used as a criterion for calculating surface roughness which is effective for differentiating these classes. The change types are categorised using information of the land cover, height and area of compared segments. Figure 2-4 below shows the categories of change derived from these factors and figure 2-5 shows the threshold definitions used to achieve final results from start of the procedure used in the research.

Categories	Former period	Later period	Change of height	Changed of area
Changed building	Building	Building	Yes	No
Newly built from existing building-to-building	Building	Building	Yes	Yes
Newly built from non-building-to-building	Vegetation/ground	Building	Yes	Yes
Demolished building	Building	Vegetation/ground	Yes	Yes

Figure 2-4: Change categories by Teo & Shih (2013). Classification was based on the land cover, height and area of segments.

No	Items	Thresholds	Description
1	Height	3 m	To detect the above-ground objects in nDSM
2	Window size	2.5 m × 2.5 m	Window size for the erosion and dilation kernels
3	Small area	50 m ²	To remove small regions in the nDSM
4	Flatness	15°	To extract those pixels with small gradients from the region
5	Roughness	40%	If the percentage of large gradient pixels in a region is smaller than the threshold, then that region is treated as vegetation
6	Area difference	50 m ²	If, after calculating the difference between two periods, the area is larger than this threshold, then the region in the later period is treated as a new building

Figure 2-5: Classification thresholds for change detection by Teo & Shih (2013).

A reported 80% accuracy was achieved with this approach with most errors attributed to areas with low vegetation roughness and small areas.

Xu et al. (2013) used ALS data from two epochs to detect changes automatically. This approach focuses on the detection and classification of a wider variety of changes found in multi epoch ALS dataset by deriving and then using surface separation values. The method accounted for errors caused from the registration of the data, which sometimes leads to false changes. Based on this, rules were defined to take into account the minimum size of real changes on the map. Results show 80% accuracy in correctly classified buildings.

In a different development, Hebel et al. (2013) moved from the classical difference methods and adopted an approach which also considers the position of the scanning sensor in detecting changes. The concept was adopted from the Dempster-Shafer theory. They also highlighted the contributions of the point density and point positioning accuracy to the minimum size of detectable changes. These factors were modelled using certain parameters (λ , c , κ) which describe the fuzziness of the laser points. An implementation of this approach involved an on-the-fly change detection which supported on-board processing by allowing the ALS sensor to gain real time access positioning systems and reference raw data for comparisons.

2.3. Working with 2D maps

In comparing LiDAR data with maps, cartographic rules and regulations must be considered but a suitable platform for comparison must first be created. Vosselman et al., (2004) identified the need to carry out segmentation followed by classification of the segments on the laser data. This leads to comparing building segments with buildings on the map. After achieving an overall accuracy of 90% for classification, results prompted the need to analyse further errors that appeared after change detection, hence, it was resolved that other sources of errors can accrue from:

- Generalisation of objects on the topographic or 2D maps, whereas the laser data maintains original object structure. Morphological operations (dilation and erosion) were employed to effective ends to minimise differences that may have been caused by generalisation.

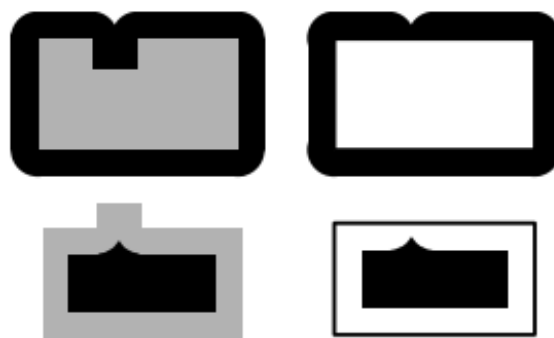


Figure 2-6: Check for intrusion of laser segment by using the dilated laser segment (top left) and fitting to the generalised database object (top right); for protrusion by using the eroded laser segment (bottom left) and fitting inside a generalised database object (bottom right). Source: Vosselman et al., (2004).

- Random data noise inherent in the separate datasets used for comparison. The morphological kernel used was enlarged in order to accommodate the tolerance in change detection.
- Systematic errors observed by identifying misalignments between similar objects on the separate datasets. This shift was corrected by re-aligning the object on the database before the implementation of change detection.

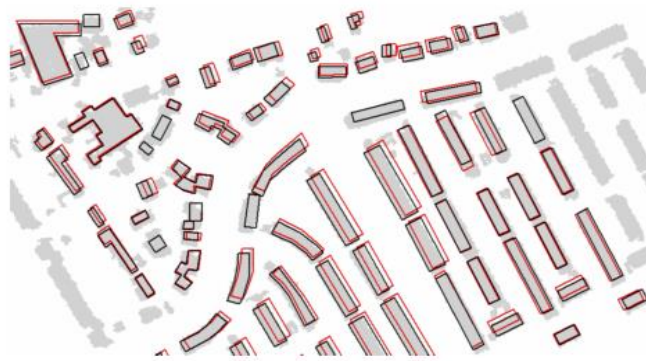


Figure 2-7: Systematic offsets that may exist between building segments in a laser dataset (grey) and a vector map (red lines). Source: Vosselman et al., (2004).

- Object selection, here certain objects are omitted as part of the mapping rules for the topographic maps, objects that fell within this category were removed on the segmented data in accordance to the specifications of the topographic mapping rules.



Figure 2-8: Segments falsely marked as new buildings (red) which were in fact omitted in the map due to mapping rules. Source: Vosselman et al., (2004).

As a result of these considerations, real changes are efficiently discriminated from false changes, meaning that the change detection process already proves to be valuable for assessing quality of the topographic maps. In a separate study, Freire et al., (2014) introduced stringent mapping standards in assessing buildings derived from very high resolution satellite imagery. They considered various assessment measures including geometric deviations from reference maps being measured with cartographic constraints at various map scales. It was observed that the geometric quality of small scales map easier satisfied the strict standards for planimetric deviation than large scale maps.

2.4. Quality of LiDAR data

In as much as some of the rules in a map production process are considered when analysing changes, there still exist challenges that are inherent in the use of images and LiDAR data. Questions about how good the reference data is need to be answered. For LiDAR data, it is primarily stated that interpreting and

detecting changes could be affected by poor reflection from water logged surfaces and occlusions (Oude Elberink and Vosselman, 2011). These amongst several other factors can affect the quality of point clouds used for analysis.

Vosselman (2008) adopted measures to analyse point clouds accuracy by checking deviations of extracted ridgelines from overlapping strips. To achieve this, the method focused on areas with overlapping strips, segmentation was implemented to detect roof planes on the point clouds. Then, the ridge lines of the roof planes are derived by computing the intersecting lines from the roof planes. These lines in overlapping strips are consequently compared to determine the offset between them.

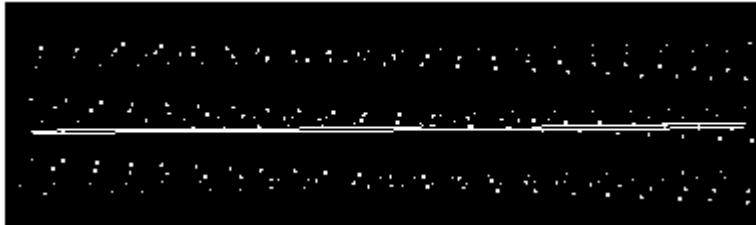


Figure 2-9: offsets between identical ridgelines in an overlapping strip. Vosselman (2008)

Results from the research proved that planimetric standard deviation of 2cm is achievable in strip adjustments of point clouds.

In a similar investigation, Van der Sande et al. (2010) proposed a new approach in which planar features are extracted from AHN-2 data and used for strip adjustments and accuracy assessment. The strip adjustment was simply done by evaluating the systematic and random errors in the data by computing distances between identical planar features in overlapping strips. Results reveal vertical displacements of up to 4cm and horizontal offsets between 2cm to 34cm.

In another development, Vosselman (2012) cemented on the accuracy of outlining objects from point clouds by proving a maximum standard deviation of 5cm for the planimetric accuracy. Anil et al. (2013) also used deviation analysis to assess a building model derived from point cloud data. The deviations between the model and point cloud are visualised at every point and represented with a colour scale in order of magnitude. These investigations have proven that point cloud data are of reliable horizontal and vertical accuracies and such are appropriate for reference data.

2.5. Quality assessments in change detection

Gong et al., (2008) have listed several factors that affect change detection results, these factors have been attributed to cost and time constraints, terrain complexities, the algorithms adopted, operator's competence, quality of registration and calibration and the quality of reference data used. Considering these complexities, seeking appropriate measures for quantifying differences in maps and how they can reflect change remains to be fully investigated.

Van Coillie et al., (2008) used number of segments that have centroid in reference polygons, difference in total area, difference in total perimeter, difference in shape complexity and average distance between edge

pixel and reference pixel, but this was applied to the evaluation of segmentation quality. Khoshelham et al., (2010) also used a pixel based metrics for accuracy assessment of methods used to detect buildings. These approaches are rudimental in thinking on the way of quantifying differences and classifying them to reflect map quality and object change.

3. PROCESS IMPLEMENTATION

The chart below provides an overview of the general process involved in achieving the goal and objectives of this research.

- a) Segmentation and classification of point clouds: Segmentation involves detecting planar faces. Objects derived from segmentation will need to be grouped into classes. Several methods exist for classifying segments. The method by Xu et al. (2014) was implemented and is deemed appropriate as it achieves a 97% classification accuracy. This stage is important because classified segments provide the avenue for extracting points that fall in the classes that are needed for comparison, and in this case, buildings. These processes have already been executed in the data provided.
- b) Extraction of building outlines: Extracting outlines from point clouds is a prerequisite for comparison since the base map is a 2D vector map. Identifying an appropriate algorithm for outlining is the task here.
- c) Vector overlay operations: The 2D map is introduced at this stage and overlay operations are used to identify deviations in the datasets.
- d) Analyse deviations: Deviations derived from the overlay operations are split into two types based on the size of changed objects on the map, the two types of deviations include:
 - i) Small Differences: These differences are analysed statistically by computing the vertex-line distance of identical objects from the two datasets. They reveal the geometric accuracy of the map. Details will be discussed in chapter 4 of this report.
 - ii) Large Differences: Large differences are analysed to investigate for real changes. These changes may have been instigated by construction activities, occlusions, sun shades etc. The changes are interpreted and classified. Details will be reported in chapter 5.

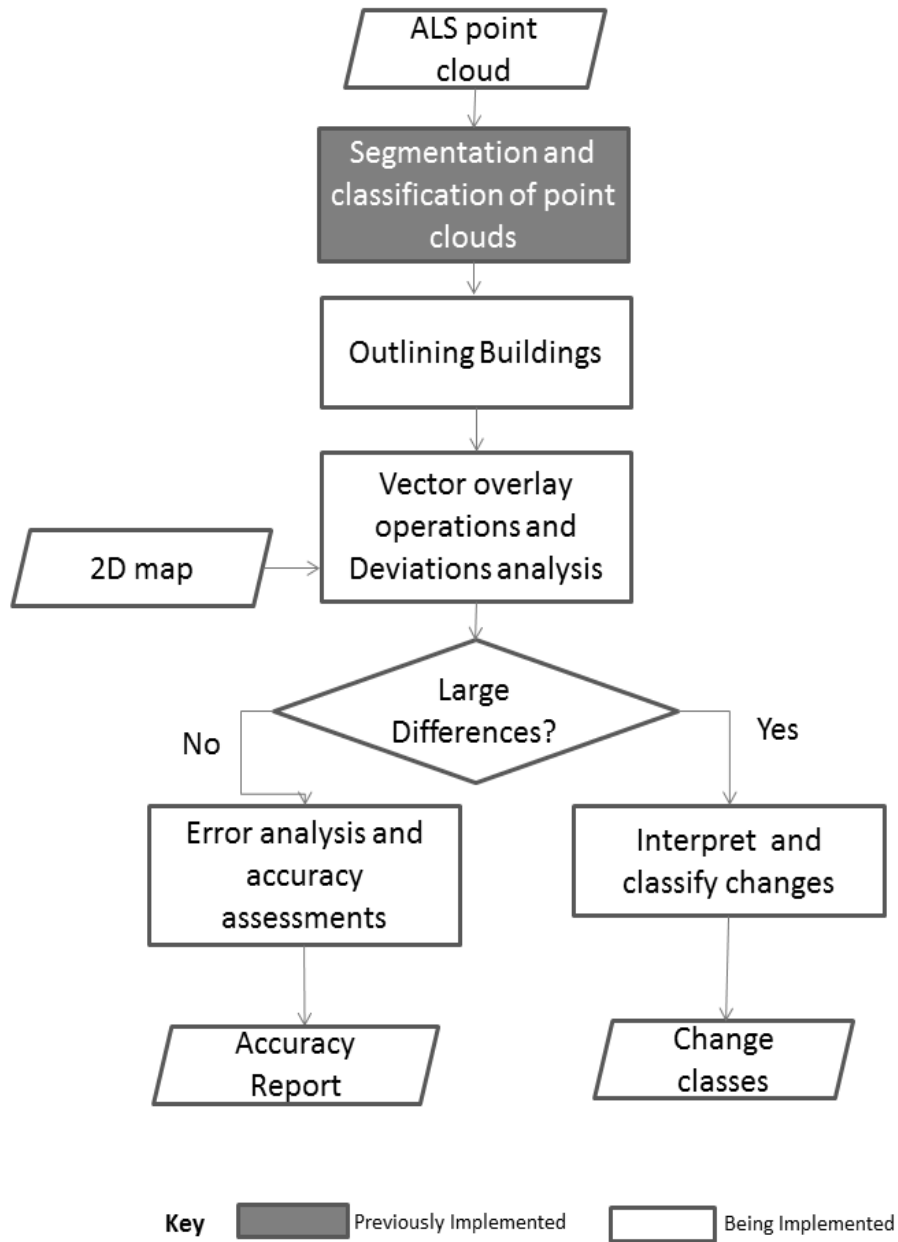


Figure 3-1: Flow of processes in analysing change

3.1. Data

An area around the Rotterdam central station is used in the research. The selected region covers an area of approximately 1 square kilometre (1km²) with 255 building polygons employed for investigation. The data sets used in the thesis are:

- a) Classified point cloud data of part of the city of Rotterdam at an average point density of 30points/m².

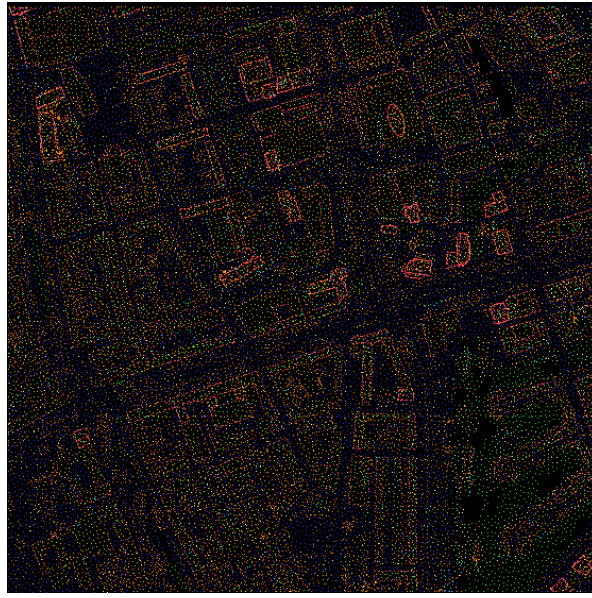


Figure 3-2: Classified point clouds covering the study area, the different colours represent the classes derived from the classification process.

- b) Building outlines of the city of Rotterdam from the Dutch base registry BAG for the year 2010.



Figure 3-3: 2D map of the study area clipped from the Dutch registry BAG.

3.2. Data Preparation

3.2.1. The point clouds

The point cloud data for the city of Rotterdam was acquired in 2012, which makes it more recent than the map dataset. Considering the high planimetric accuracy (as reported by Vosselman (2012)), the point cloud serves as a suitable reference dataset for comparison with the 2D map.

3.2.1.1. Selecting building components

The classified point cloud originally contains seven labels (wall, roof, roof elements, vegetation, ground, water and undefined objects). Since the comparison is implemented just for buildings, there is the need to extract only building components from the point cloud data; this leads to identifying only classes that are connected to buildings. In selecting building components, this motive is duly achieved using the labels associated with buildings only which include walls, roofs and roof elements.

3.2.1.2. Growing Segments

Growing segments involves implementing a connected component analysis on the selected labels for buildings. Building segments are created based on similarity of points. The distance metric which determines the Euclidean space in which the proximity of the points will be considered is pre-set to 2D since the resultant operation will be compared from the orthogonal perspective. The components are grown in tile-wise manner as seen in figure 3-4 below.

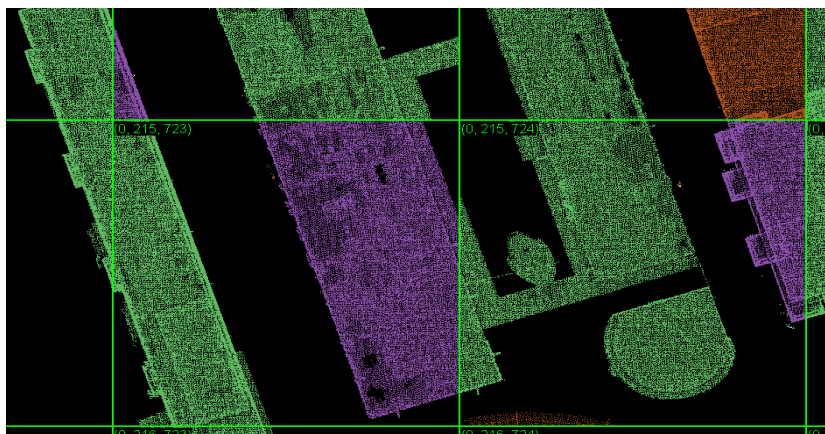


Figure 3-4: Tile-wise results after growing building segments. The different colours represent the separate building components in each tile.

3.2.1.3. Block Segments

With a tile-wise representation of the building segments, there are disjointed building components, especially for features that lie across tiles. Combining the segments resolves the discontinuity in objects by merging components across tiles using boundary zone for searching across tile borders. A region of 1m is used as the search range for bordering points. This results in a complete block with building segments in complete patches.

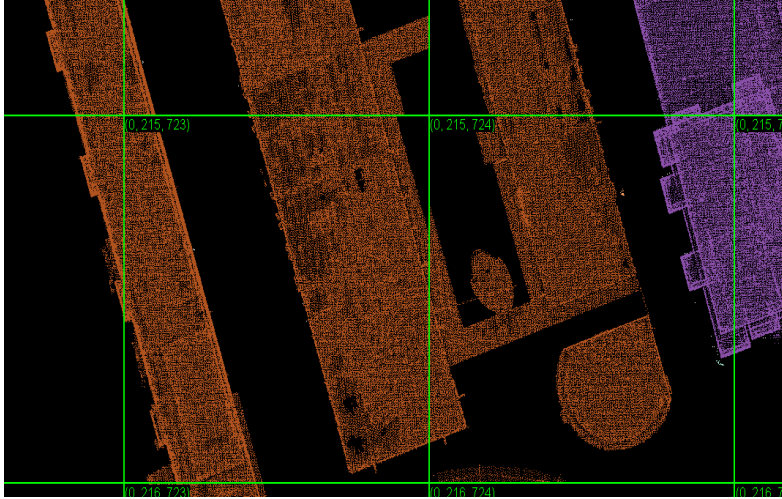


Figure 3-5: Result of block segments operation executed after the grow segments function

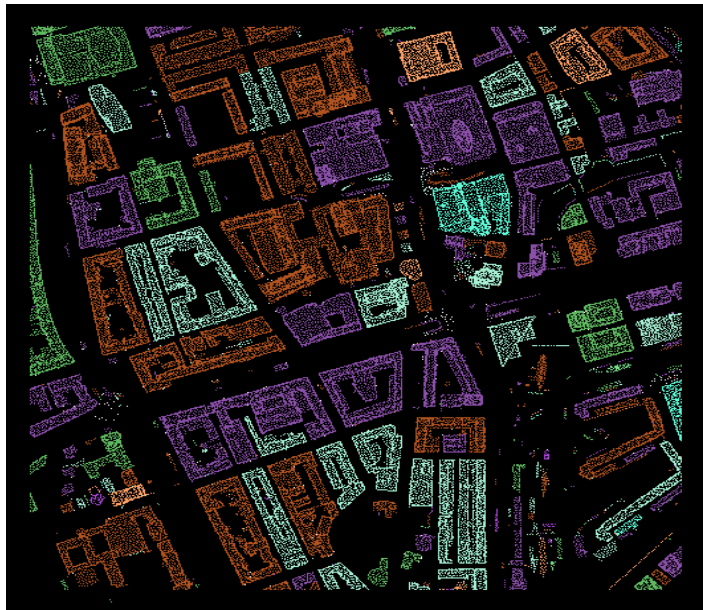


Figure 3-6: Block segments result of study area. Each building block represented in different colour.

3.2.2. The map data

The 2010 version of the BAG datasets is used here. The BAG is a key register originally composed of two key registers in the Netherlands and is managed by all municipals. These two key registers are the Key Register of Addresses (BRA) which holds information on towns, street names and house numbers and the Key register of Buildings (BGR) which holds data on buildings, premises, permanent locations and mooring. They are combined into one considering the inevitability of having one existing without the other. This makes the BAG registry a key register of Buildings and Addresses (Ellenkamp & Maessen, 2009). The BAG dataset represents all buildings at residential units and contains certain attributes such as the year of construction, the number of floors, the status, etc. The national requirement for the absolute point accuracy for the BAG is 20cm.

3.2.2.1. Updating Attributes

The dataset contains buildings at all levels. The levels here refer to the number of floors each building has. The field containing this information is updated, all underground building are selected and excluded from further analysis, since the ALS sensor will not capture underground features. This is to ensure that comparison of the datasets is done at the same perspective in order to minimise the inclusion of false changes.

3.2.2.2. Aggregate Polygons

For an effective comparison to take place, the polygons in the BAG datasets are processed to conform to the patches on the point cloud. Originally, the buildings are partitioned in smaller blocks on the parcel level; these blocks are subsequently merged to represent whole units.

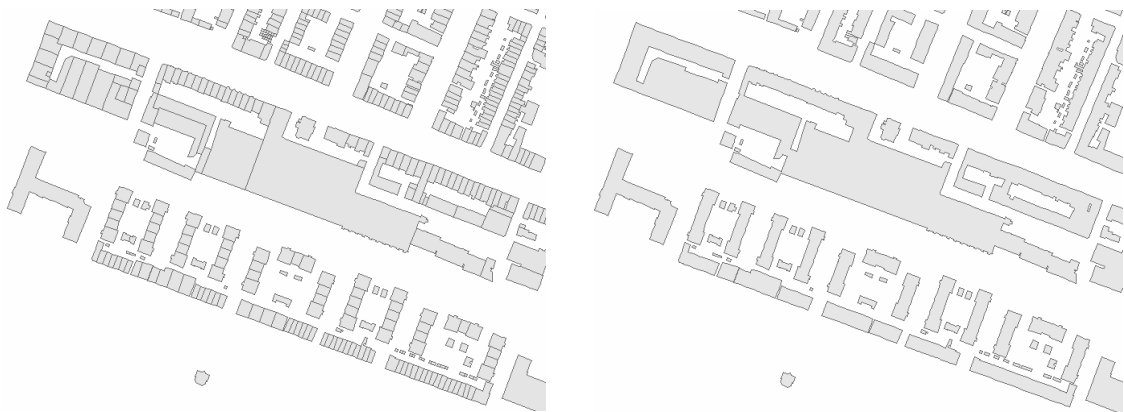


Figure 3-7: Polygons before (left) and after (right) aggregation.

3.3. Building outlines from point cloud

An outlining procedure has been adopted here which is based on an aggregation of a cluster of points. Outlines are derived from the point clouds in order to be able to precede with the overlay operations on the datasets. Point aggregation is a generalisation procedure which simplifies cluster of points into polygons. Polygonal boundaries are wrapped around the point clusters by using a proximity threshold to determine points that are considered within a cluster. Results are similar to those obtained from using concave hull/alpha shapes algorithms. This procedure involves three distinct stages: building a Triangulated Irregular Network (TIN), clustering based on proximity constraints and constructing polygons around clusters.

- Building a TIN: A TIN is built on the points using a Delaunay triangulation method. This method maximises wide angles between neighbouring points and connects them in triangles ensuring that no point is left inside the circumcircle of any triangle (Wikipedia, 2014). A network work of interlinked triangles is derived and each triangle represents a plane with a continuous surface.

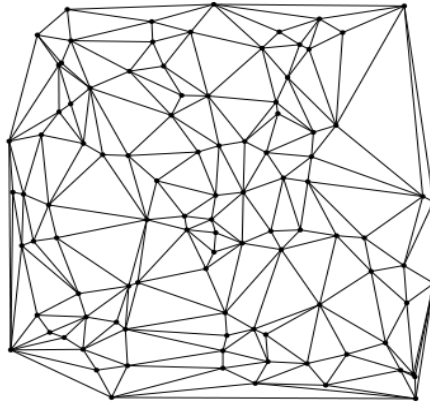


Figure 3-8: An example of Delaunay triangulation of a set of random points. (Source: Wikipedia, 2014)

- Clustering: An aggregation distance is used as a proximity criterion to find clusters. The lengths of sides of the triangles in the TIN provide values for this evaluation. Due to the random spatial distribution of the point clouds as a result of irregular point spacing, the aggregation distance is tested within a range of values in order to find a compromise between having too many holes in the polygons and over generalisation of the edges. A convenient value of 0.6 meters was used in the process to obtain satisfactory results.

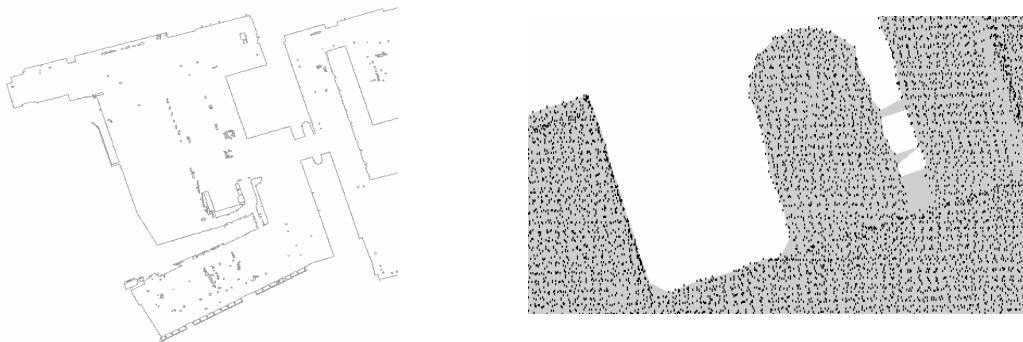


Figure 3-9: over perforation of polygons caused by small clustering threshold (left) and over generalisation due to large clustering threshold (right)

- Constructing polygons: with the clusters determined, polygons are drawn around clusters connecting most of the vertices on the outside of the clusters.

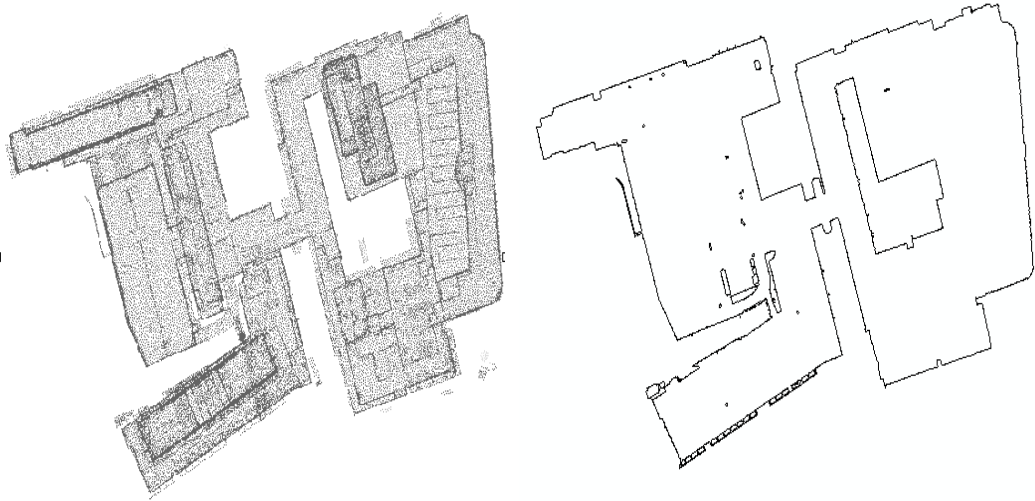


Figure 3-10: Point clouds segment for a part of the block (left) and the resulting outline for a building polygon (right)

3.4. Overlay Analysis

The symmetrical difference is performed as an overlay operation on the two datasets. Having two sets A and B, the symmetrical difference is given mathematically as:

$$A \Delta B = (A - B) \cup (B - A)$$

This operation results in portraying the differences between both vector datasets. A tolerance value of 0.5m is used to minimise the effect of noisy objects. This value (0.5m) is chosen after several iterations ranging from 0 to 1m. Any value higher or lower leads to highly reduced change polygons or continuously connected polygons respectively, which can make the interpretation of changes difficult, for example, a low tolerance value will lead to having polygons that are highly connected leading to a high number of objects with mixed properties. Figure 3-11 below shows the difference polygons derived by using symmetrical difference overlay analysis.

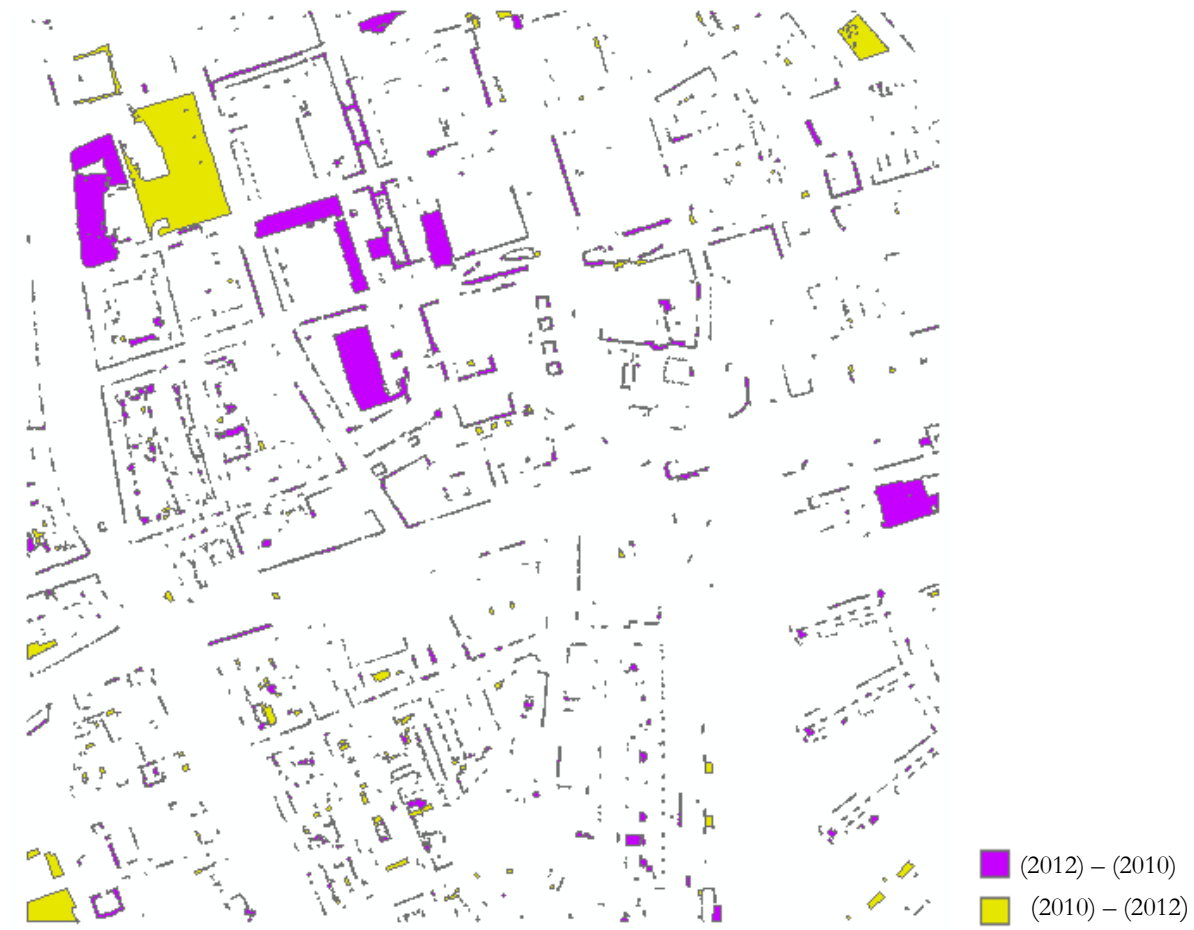


Figure 3-11: showing the differences in polygon datasets using symmetrical difference overlay analysis.

3.5. Distinguishing the kinds of changes

A clear distinction between the kinds of changes identifies what kinds of deviations are directly linked to the quality of the map outline and those that are linked to real changes.

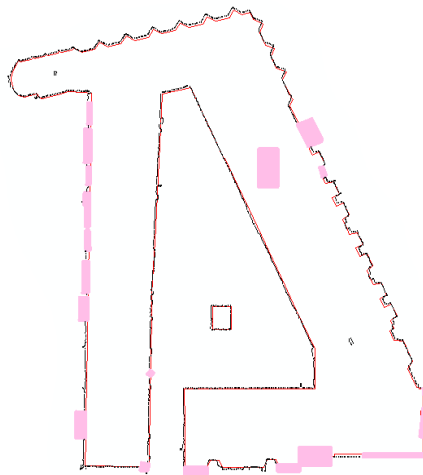


Figure 3-12: Use of bounding boxes (pink) with threshold values to distinguish points with large differences from points with small differences (black dots). The red line represents the map outline

In distinguishing these changes, the first approach is to look at the characteristics of objects on the area being observed. The size of the smallest kind of real change is the primary indicator. In addition to the size, the length and width of the extent of the changed object is considered because, only the size of the changed object might not be a completely decisive indicator in some cases, especially when the object is very large or very small. For example, a building side of 50 meters long with an observed extension of 20cm will translate to an area of 10 square meters, whereas in reality an extension of 20cm construction activity is not feasible. Hence the width and length of the changed object is important, which means, a rectangular bounding box (as shown in figure 3-12) around a changed object becomes useful for further analysis.

After carefully observing changed objects in the study area by looking at their characteristics on some aerial and street images from Google, it was observed that all real changes were longer or wider than 1m. Therefore, 1 meter is used as a selection criterion to filter out points that fall within a bounding box that is longer or wider than the said threshold. With that in place, only the vertices of points from the point cloud outline that are not within the selected bounding boxes are compared to the 2D map outline.

4. DETERMINATION OF GEOMETRIC ACCURACY OF THE 2D MAP

The geometric accuracy of the 2D map is determined by statistically analysing the small differences found in the map. It is generally expected that the representation of an object on one dataset should be the same as the representation of the same object on another dataset. Since the BAG polygons are generated from aerial photographs, the polygons are expected to coincide with the polygons generated from the LIDAR point clouds as they both represent the roof outlines of buildings. However, deviations are inevitable and are observed to be caused by several factors such as the uncertainties caused by the processes in the separate building outlining processes, the quality of the reference data (LIDAR point clouds) and actual construction on ground.

4.1. Finding the Geometric Accuracy of the map

After filtering out the large deviations caused by real changes, the small deviations are used to determine the accuracy the map. Using the point cloud data as reference requires that the uncertainties inherent in the outlining process must be modelled. These uncertainties as observed by Vosselman (2008) are due to the point distribution around the outline of the object and the location accuracy of the laser objects. The other differences are those that are inherent in the map. In summary, the differences between the map and the building outlines in the point cloud are caused by:

- a) Uncertainties in outlining due to point spacing.
- b) Uncertainties in point location.
- c) Uncertainties in the map itself i.e. map accuracy.

Knowing that these differences can be measured by looking at the deviations, if the uncertainties in the point cloud elements are determined, then the map accuracy can be ascertained.

4.1.1. The uncertainty in outlining because of the point spacing

The uncertainty in outlining due to the point spacing refers to the effect of the point distribution on the outline of objects in the point cloud. To determine this effect, an experiment is carried out on a patch of point clouds taken from a relatively flat terrain in the scene. A relatively flat surface is used so that the point distribution on that surface will be more or less uniform. A line is then drawn across the patch, the outlines are modelled relative to one side of the line, and the deviations are computed to determine the effect of the point distribution on the outline. This experiment is repeated for each side of the line and another line is drawn at every five degrees until a full circle is achieved so as to have sufficient samples for the experiment. A total of 72 lines were used. Figure 4-1 below shows how the simulation is implemented.

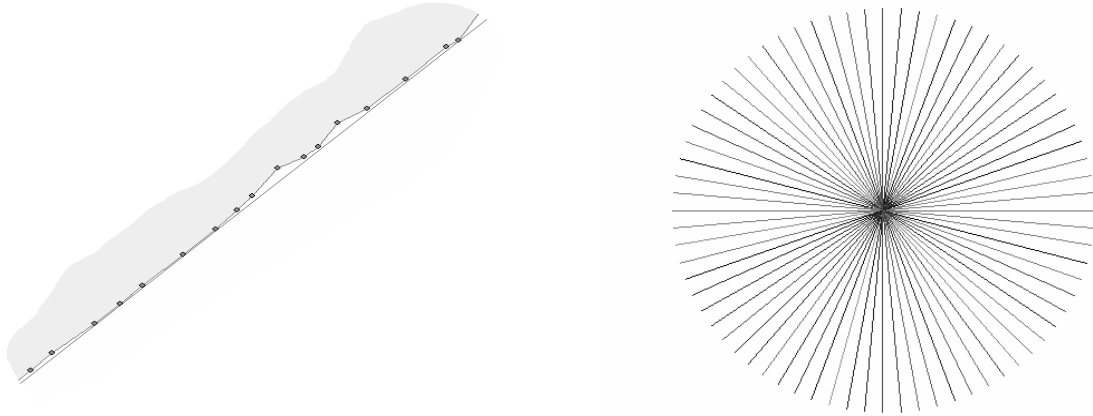


Figure 4-1: Sample of the effect of point distribution on the outline of an object (left) and the line turned through every five degrees resulting in 72 lines (right)

In figure 4-1 above, the points are derived from the vertices of the outline, and the straight line is an arbitrary building outline, the perpendicular distances from the vertices to line are computed to determine the deviations. With this simulation, there is a systematic effect which is represented as the bias (\bar{d}) of the observations and this is computed as the mean of the deviations to be 5cm. The standard deviation ($\sigma_{\text{pointspacing}}$) is also derived to be 5cm.

4.1.2. The uncertainty in point location

The uncertainties in point location refers to the planimetric accuracy in the position of the laser points. Vosselman (2012) developed a method which assessed the planimetric accuracy of mapping objects in a point cloud and this method was verified by checking the shifts in the ridge lines of gable roofs in strips overlaps. The standard deviation ($\sigma_{\text{point location}}$) of the point clouds was derived to be 5cm.

4.1.3. Finding the differences

The differences between the outlines are calculated by measuring the point to line distances from the vertices of the outline of the point cloud to the map outline. The equation for the point to line distance measures the perpendicular distance from a given point to a line and is given as:

$$X \cos \alpha + Y \sin \alpha - d = 0$$

Where:

d is the distance from vertex to line,

α is the azimuth of the line and

X and Y are the coordinates of the points.

This equation measures the distance from each vertex in the point cloud outline to the adjacent map outline, a search radius of 1m is used as points beyond this threshold translate to large changes. The distance is corrected for a systematic effect derived and described as the bias (\bar{d}) estimated in section 4.1.1. This is expressed as:

$$e' = d - \bar{d}$$

Hence, the overall accuracy is expressed as the sum of the three accuracy components:

$$\sigma_{e'}^2 = \sigma_{\text{point spacing}}^2 + \sigma_{\text{point location}}^2 + \sigma_{\text{map}}^2$$

Given that the left hand side of the equation has been derived from measurements made from the point to line distance calculations, and the point spacing and point location related uncertainties have been estimated, the estimate for the map accuracy remains the only unknown variable and is then easily calculated in the equation. Using a total of 255 building polygons from the study area, the errors from all observations are computed and the overall accuracy of the map (σ_{map}) is derived to be 25cm.

4.1.4. Assessment of the accuracy determination method

The method used to assess the geometric accuracy of the map is tested to ascertain its robustness. This is achieved by splitting the study area into four blocks and each block is processed independently to determine the accuracy of the block. It is expected that the results will be similar if the method is reliable. Table 4-1 below shows the results for the four blocks:

<i>Block Number</i>	<i>Calculated accuracy (σ_{map})</i>
Block 1	24cm
Block 2	25cm
Block 3	24cm
Block 4	28cm

Table 4-1: Results for map accuracy calculated independently for 4 blocks.

From Table 4-1 above it can be seen that the accuracy determined across blocks are close to each other. Similarity in the results proves that the method used is reliable.

4.2. Discussions of results for the geometric accuracy of map

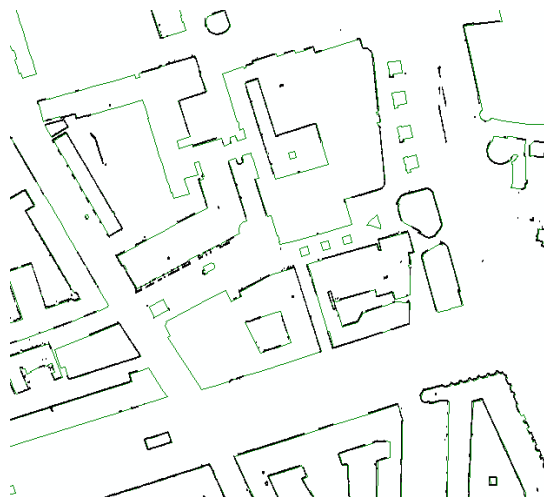


Figure 4-2: A clip of the study area showing the small differences. The black dots represent the vertices of the outline from point cloud and the green lines are the map outline.

The required accuracy was set to 20cm, but with the results obtained, it can be observed that the accuracy of the map is approximately 25cm. This has been computed using the observed differences from the representation of the datasets. Factors that contribute to the outlining of objects have been equally modelled to achieve the results. This shows that the accuracy of the map is not too far off from the national accuracy requirement.

5. INTERPRETING LARGE DIFFERENCES

Interpreting the large differences follows a supervised classification process, where samples are trained and rules are defined based on the trends in the samples. Large differences are defined by objects longer or wider than 1m. These differences are caused by objects that directly alter building outlines as a result of large deviations from the point cloud data or actual construction work. From investigating the data used for analysis, three classes are derived which represent the large differences:

- a) **Building Extension:** This basically represents object change caused by construction activities. Even though the focus is on the extensions to buildings because of already existing algorithms that detect new or demolished buildings, it is remarkable that buildings and buildings extension share identical properties in the point cloud.
- b) **Sunshades:** These kinds of changes are characterised as small attachments to buildings, which are not building extensions, balconies also fall into this class. They are usually not represented in map outline because cartographic representations from the aerial images often dwell on roof impressions and sometimes consider sunshades as temporary structures. Segmentation and classification algorithms easily detect these features as significant parts of buildings thereby presenting a different geometry from the map outline, which leads to changes.
- c) **Vegetation:** Vegetation originally has a different class but trees close to buildings often present different challenges for classification because their proximity easily connects them to buildings. The classification algorithms sometimes fail to recognise the separate entities hence the geometry differs, causing changes on the map.

5.1. Training Samples

The task to efficiently interpret these changes and put them into the classes derived requires selecting samples and understanding their characteristics. This leads to defining rules that can efficiently identify the objects in the map. The distribution of the points' elevation is the primary variable for such analysis. Understanding the distribution of points with respect to their heights was facilitated by first looking at the histograms for typical examples for each class. As a result, the characteristics of these objects in the point cloud are defined and used for further identification. The sample sets consists of 5 samples from each class. The typical characteristics of each class are as described below with the aid of histograms:

a) Buildings extension:

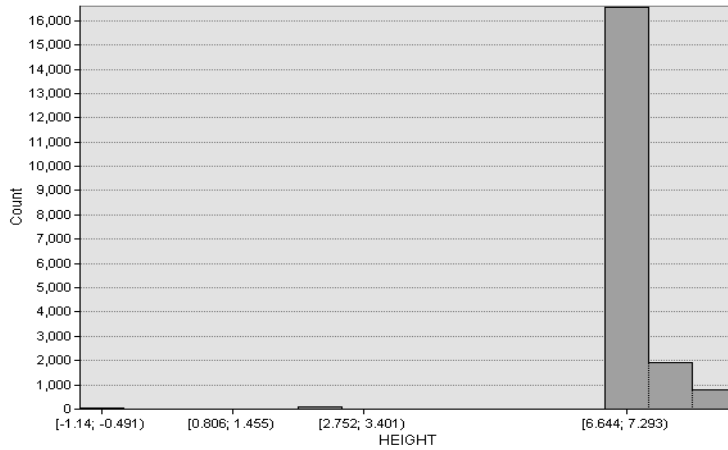


Figure 5-1: Histogram of height distribution for a typical building extension.

A typical building extension is characterised by a low number of points on the ground and a high number of points above the ground. The histogram usually shows distinct peak(s) where the points are accumulated at the roof surfaces.

b) Sunshades:

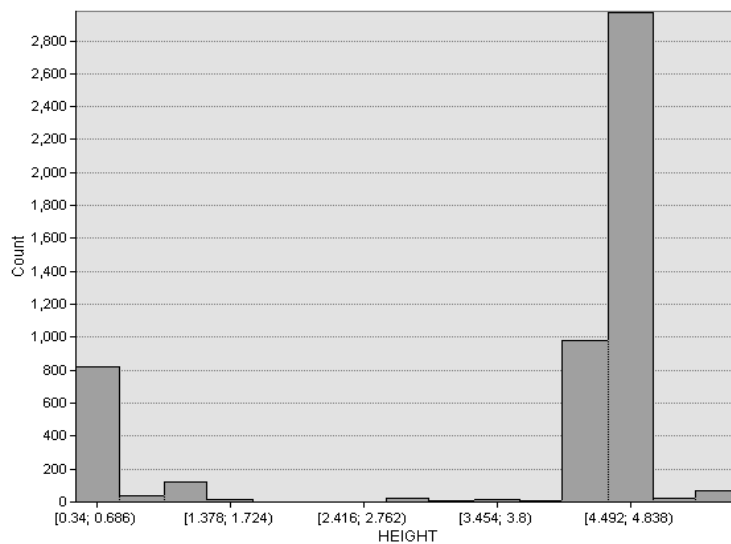


Figure 5-2: Histogram of height distribution for a typical sunshade/balcony.

Sunshades have similar histogram characteristics to building extensions; they typically have distinct peak(s) at the roof surfaces but also have a good number of points on the ground. Although their overall point count is smaller, there is often a higher percentage on the ground than building extensions. The scan angle of sensors makes it possible for more points to be captured below the sunshades, and since they typically will not have enclosed walls, penetration to the ground is improved.

c) Vegetation:

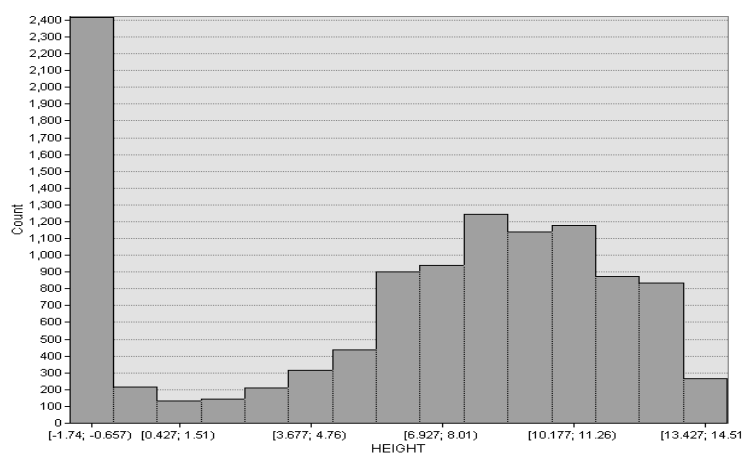


Figure 5-3: Histogram of height distribution for a typical vegetation class.

The histogram for vegetation shows a high amount of points on the ground and a good number spread across the entire range as well, but they typically have low point counts. More bins contain data for vegetation class.

5.2. Statistical measures

With the patterns of the classes observed from the histograms from the training sets, certain measures are defined to describe these characteristics of the classes. These measures will be used to define rules upon which the classification of all other polygons representing the large differences will be established. A first look at using basic measures such as mean, standard deviations and variances proved to be insufficient for describing the classes because of the slightly complex behaviour of the distribution of the height parameter. An approach which tries to use mathematical expressions to describe the separate histograms as much as possible becomes the most likely solution for classification. Based on this notion, the following measures were considered and utilised:

a) Number of bins with significant percentage of data:

Derived from the histogram's classes, the number of bin with significant percentage of data is used to define those classes that have a significant amount of points. This tends to minimise the effect of noise from other objects that may interfere with the classification of a particular object.

Two factors are used to determine this measure; the total number of bins and the significant percentage value. The total number of bins is 15 for all classes. This is chosen as a means of normalising the data between classes. This was derived after iteratively looking at the histograms of the samples. Histograms from 15 to 20 bins vary less in appearance and structure, 15 was then chosen as a convenient value that balances between having an over division of classes and under representation of classes.

The second factor, the significant percentage value was visually determined by observing the histogram samples. Selecting bins above 5% leads to over reduction in bin count and loss of some

useful data. Values from 2% to 4% show little variation in test results for the classes, so 4% is used as the constant for calculating number of bins with significant percentage of data. This implies that any bin with less than 4% of total point count is considered insignificant for classification purpose.

From the samples used, the following results show the behaviour of the classes with regards to bin count:

Sample class	Number of bins with significant percentage of data (4%)
Sunshade1	2
Sunshade2	3
Sunshade3	2
Sunshade4	3
Sunshade5	9
Vegetation1	9
Vegetation2	8
Vegetation3	4
Vegetation4	8
Vegetation5	8
Building extension1	4
Building extension2	3
Building extension3	4
Building extension4	6
Building extension5	4

Table 5-1: Number of significant bins for 5 samples in each class.

From Table 5-1 it can be seen that the vegetation class is easily detectable as it contains more bins because of its point distribution, the distribution ranges from 4 to 10 or even more. Sunshades have lower bins because points are distributed on ground and sunshade roofs with little elsewhere. For building extensions, the values vary from 3 to 6, this could be as a result of multiple story extensions, but in general the bins will not be as many as those in vegetation class. There are exceptions in the behaviour of some samples, like in “Sunshade5”; this will be discussed in section 5.3.

- b) Entropy: Entropy measures the degree of randomness or variation of a variable. Height distribution in the classes exhibit varying degrees of variation and as a result, entropy is used to investigate the behaviour of height distribution in each class. Shannon (1948) mathematically defined entropy as;

$$H = -\sum p_i \log p_i, \text{ the entropy of a set of probabilities from } p_1 \text{ to } p_n.$$

For this specific case, the probability is calculated as the number of points in a class/bin divided by the total number of points in the sample. Table 5-2 below shows the entropy values calculated for each sampled object.

Sample class	Entropy value
Sunshade1	0.463
Sunshade2	0.452
Sunshade3	0.169
Sunshade4	0.424
Sunshade5	0.972
Vegetation1	1.063
Vegetation2	1.049
Vegetation3	0.745
Vegetation4	0.950
Vegetation5	0.948
Building extension1	0.781
Building extension2	0.233
Building extension3	0.581
Building extension4	0.691
Building extension5	0.943

Table 5-2: Entropy values for 5 samples in each class.

Entropy values for sunshades from the samples are averagely below 5, buildings show a wider range of values but in most cases higher than sunshades but lower than vegetation which ranges from 0.7 and above. Again the peculiar sunshade5 will be discussed later.

- c) Ground ratio (Gr): The ground ratio is defined to adequately describe classes based on the points on the ground. It is calculated still from the histogram classes with the underlying assumption that, majority of the ground points in a given sample will fall in the first bin of the histogram. This is because the first class in the histogram contains values around the minimum. This is simply expressed as:

$$\text{Gr} = [\text{no. of pts. in the first bin} / \text{sum of points in other bins}] \times 100$$

From this expression, the ground ratios for the samples were generated and are shown in table 5-3 below:

Sample class	Ground ratio
Sunshade1	31.0
Sunshade2	13.5
Sunshade3	13.3
Sunshade4	15.4
Sunshade5	03.3

Vegetation1	13.9
Vegetation2	27.4
Vegetation3	17.3
Vegetation4	32.0
Vegetation5	42.5
Building extension1	07.8
Building extension2	0.10
Building extension3	0.04
Building extension4	07.9
Building extension5	02.9

Table 5-3: Ground ratio values derived for 5 samples in each class

The ground ratio creates a good distinction between the building extension and other classes. Building extensions as expected contain lesser ground points and the values reveal values below 10 per cent. Vegetation and sunshades have higher percentages of ground points.

- d) Number of points in a sample: To further improve on the distinction between sunshades and buildings, the number of points in a sample (simply referred to as point count) also plays a significant role. From the samples taken, a threshold value was set to 18,000 points as the maximum number of points a sunshade may possess. The point count is directly proportion to the size of an object, for a small object will contain lesser point than a larger object.

5.3. Formulating classification rules

After defining the measures described in section 5.2, classes are then defined based on their properties with these measures. A combination of these measures can provide a means for distinguishing classes as their values differ in each class. The scatter plots below show the behaviours of these classes using the measures described above, this is to visually appreciate how the rules are formulated from the measures.

From the scatter plots, it can be observed that the objects form cluster patterns from the measures used. The trends can be used to specify thresholds for the class definitions. Though the measures may not explicitly segregate the classes when used alone, combining them will produce remarkable results.

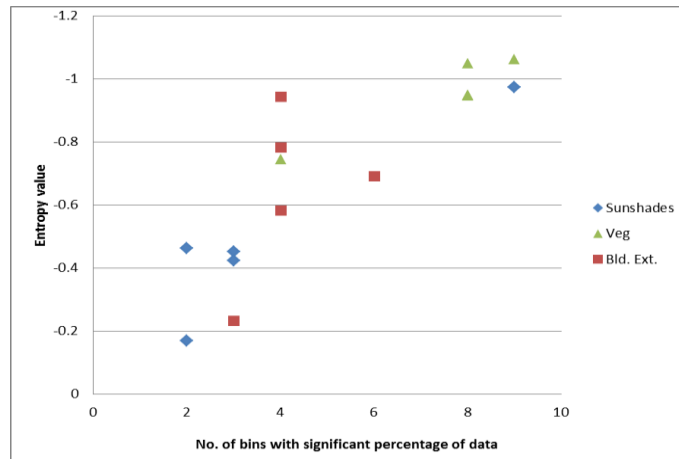


Figure 5-4: Scatter plot showing the number of significant bins against entropy values for the samples.

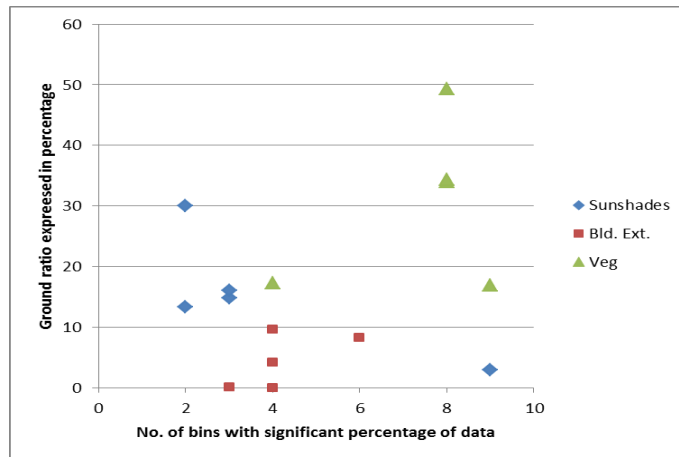


Figure 5-5: Scatter plot showing the number of significant bins against ground ratio for the samples.

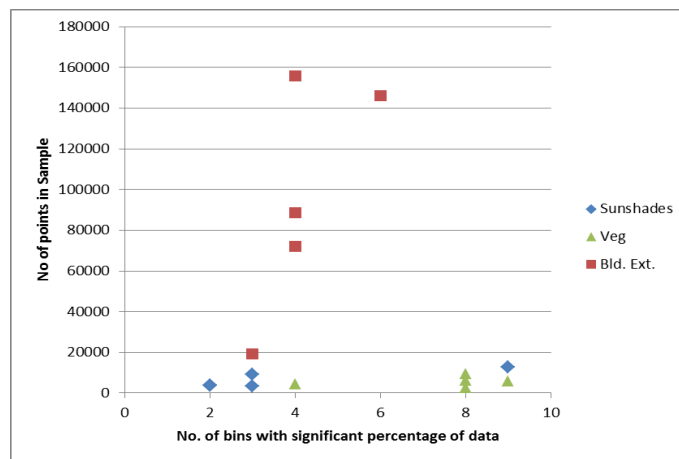


Figure 5-6: Scatter plot showing the number of significant bins against number of points in samples.

Now, addressing some outliers in the samples, it is seen in the scatter plots that “sunshade5” continuously falls in an unexpected region, where it sometimes falls in building extension or vegetation regions but its relative size and location on the map suggest it is a sunshade. This calls for a closer look at the object. The object is again observed carefully and it is discovered that the polygon contains a great percentage of roof and wall element which could pass it for a building extension, but it is not sufficiently large enough to be an extension and contains a reasonable amount of sunshade as well. (See figure 5-7 below)

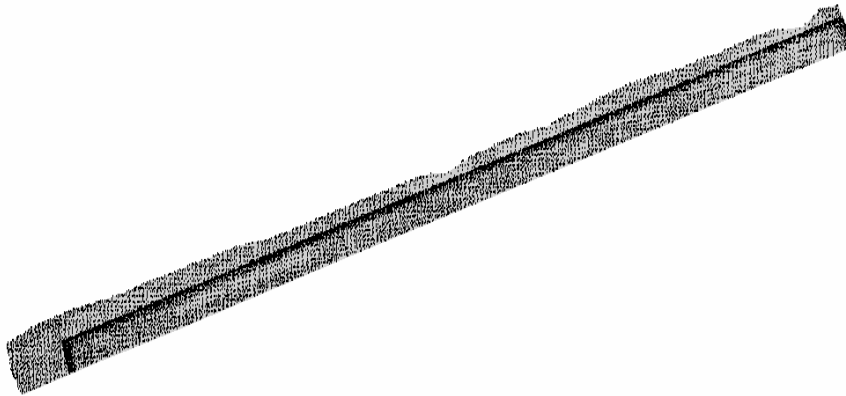


Figure 5-7: Supposed sunshade with a clear roof and wall outline inside it.

The large presence of wall and roof element was discovered to be as result of a rare operator error in the map outline. This resulted in a mixture of classes and leads to making a decision to include another class termed “Mixed objects” which describes this kind of instance and many more.

Also in another separate instance where “vegetation3” often falls in the region of sunshades in the scatter plots, a closer look reveals a peculiar case where the tree canopy is very dense making the points to cluster around the crown and giving it a planar impression. This also results in reduced penetration, thereby reducing the amount of points that are expected on the ground making it behave like a typical sunshade.

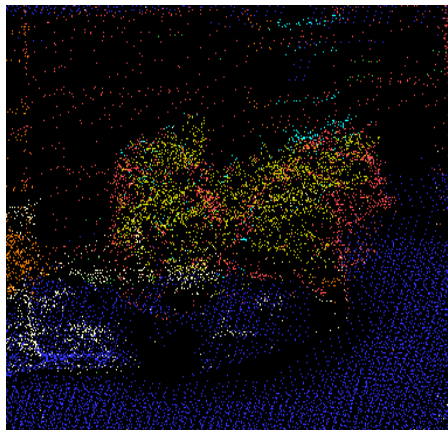


Figure 5-8: Dense tree crown (orange and lemon points) causing sparse distribution of ground points (blue) below it leaving gaps (black space).

To accommodate cases like this, the threshold for the number of bins for vegetation is adjusted to cover a wider range of bin counts in that class.

Using the values from the tables and scatter plots for the samples and also considering the special cases listed above, the final classes and classification rules are defined accordingly. These rules are made up of a combination of thresholds derived from considering the range of values for each measure in the separate classes.

The table and chart below shows a summary of the rules used for defining classes and the algorithm used to compute the classes respectively.

	Class	Rules
1	Vegetation	Object is tagged vegetation if Entropy is greater than 0.7 and Number of significant bins is greater 4 and ground ratio is greater than 12 per cent.
2	Building Extension	Object is tagged building extension if Entropy is less than 0.9 and number of significant bins is less than 7 and ground ratio is less than 10 per cent.
3	Sunshade	Object is tagged sunshade if Entropy is less than 0.6 and number of significant bins is less than 7 and ground ratio is greater than 10 per cent and point count is less than 18000.
4	Mixed objects	Object is tagged mixed object if it is neither tagged vegetation nor building extension nor sunshade.

Table 5-4: Rules used to define classes inferred from samples.

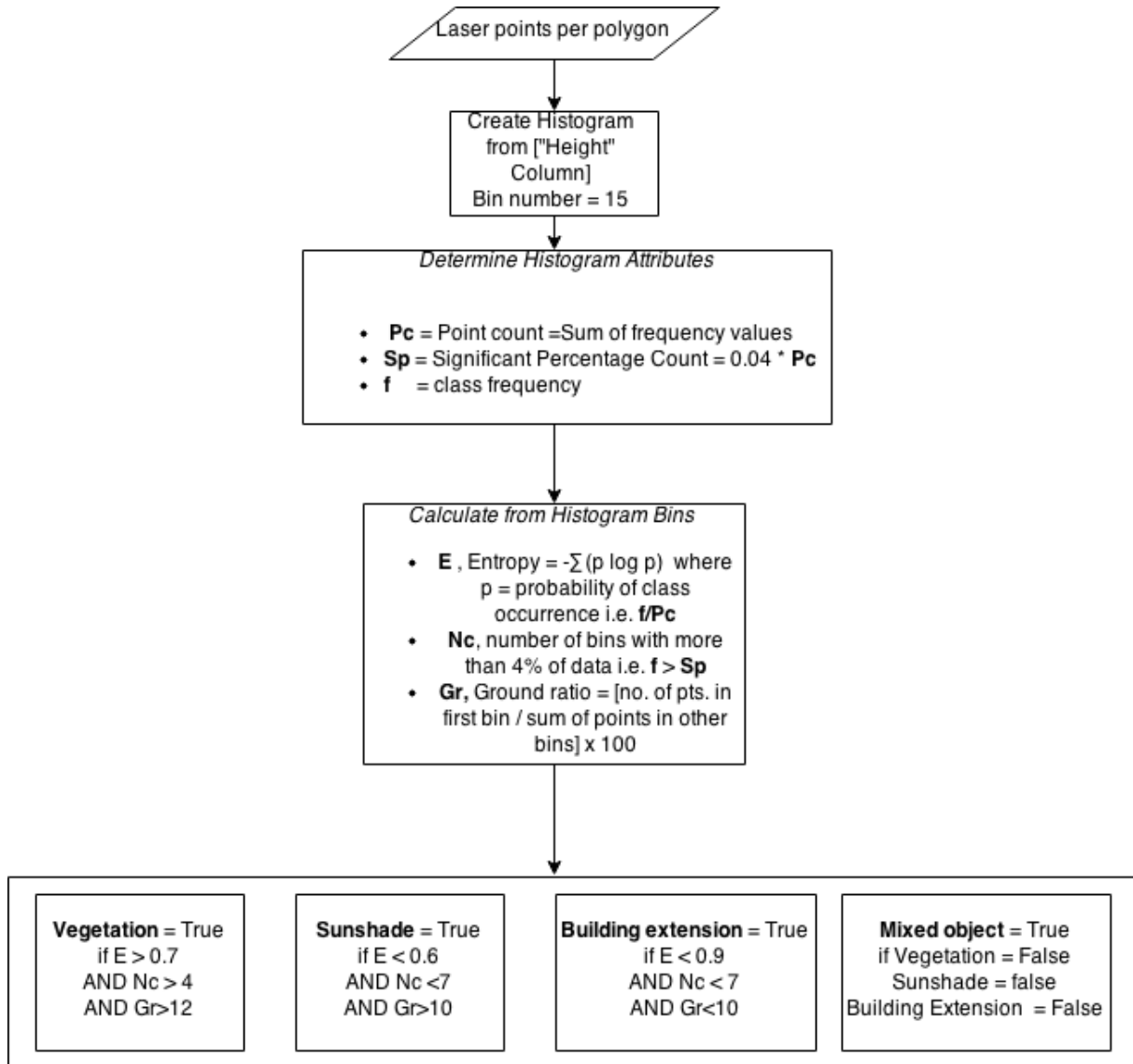


Figure 5-9: Classification algorithm for change polygons

In selecting the points per polygon, polygons are given an inward buffer of 30cm so as to minimise the effect of noise from surrounding objects. This is especially applicable in sunshades where adjoining wall elements may contribute a high percentage of laser points which in turn may affect proper classification. The 30cm offset ensures that majority of these kinds of points are not selected in the analysis. Then the classification is implemented. The classification algorithm produces labels which are assigned to all points per polygon. The points per polygon all contain the same label. To improve computation speed, the points in polygon are filtered to a minimum value. The attributes of the filtered points are transferred to the polygons (using a spatial join) to identify polygon class.

Results of the classification are shown below:



Figure 5-10: classification results overlaid on map outline

5.4. Accuracy assessment of classification

Assessing the accuracy of the classification involves comparing the results with some sort of reference data. This is often done using ground-truth information from field acquisitions. But in this case, reference data was obtained from Google earth by looking at the aerial and street views of areas where changes were perceived. A total of 74 samples were randomly taken as references and the assessment was done using an error matrix. The error matrix show the user and producer accuracies per class. The overall accuracy is computed from the matrix too.

		Reference data				Total	Error of commission (%)	User accuracy (%)
		Sunshade	Building Extension	Vegetation	Mixed object			
Classified data	Sunshade	11	1	1	0	13	15	85
	Building extension	1	11	0	0	12	8	92
	Vegetation	4	1	22	2	29	24	76
	Mixed object	6	3	3	8	20	60	40
Total		22	16	26	10	74		
Error of omission (%)		50	31	15	20			
Producer accuracy (%)		50	69	85	80			

Table 5-5: Error matrix for assessing accuracy of the classification.

An overall accuracy of 70% was obtained for the classification. Classification results are affected by a number of factors:

- i) There are instances where sunshades and buildings extensions are confused by the classification algorithm especially when the building extension is relatively smaller than the size of most sunshades. Also, concrete sunshades and balconies that are also large can easily be classified as buildings as they allow minimal penetration of the sensor data to the ground, hence the ground points are reduced making the sunshade look like a building.



Figure 5-11: A typical scenario where there is uncertainty in sunshade/building extension classification.

- ii) Mixed objects are first identified by the nature of their enclosing polygons, which tend to stretch over several entities in the scene. In some cases these kinds of objects are placed in any of the other three classes. This happens because the algorithm identifies that majority of the points contained in the polygon of the mixed class tend to conform to the attributes of the selected class.

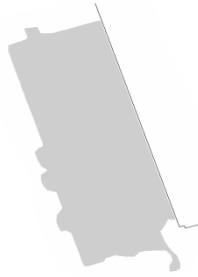


Figure 5-12: A likely “mixed object” class classified as building extension because of the overwhelming presence of building extension characteristics.

- iii) Similar to ii) above, another common misclassification occurs when a class may be classified as another when there is a huge presence of the second object class in the polygon. In principle, the classification may be correct but the nature of the polygon’s location may tend to suggest otherwise. For example, some sunshades are classified as vegetation because of the presence of overhanging trees over the sunshade areas, either class will be correct in such a case, it is left for the algorithm to choose which one is more recognised.

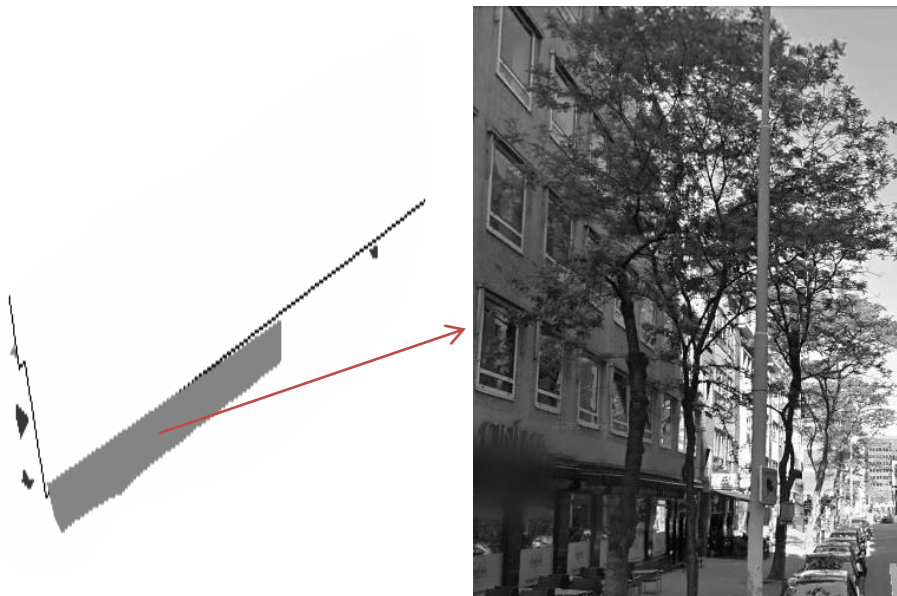


Figure 5-13: A supposed sunshade classified as vegetation because of the presence of overhanging trees.

These factors played a role in achieving a lesser accuracy, however it has been observed that there is reasonable justification in the results of some of the objects classification as seen from the instances mentioned above. Notwithstanding, there are possibilities of improvements which will be discussed in section 6.2.

With the results from the error matrix table, it becomes necessary that the classes obtained are further separated into relevant and irrelevant changes; this is in line with one of the objectives of this research. The need for this is to guide the user/operator to regions on the map where the changes are actually relevant for updating the map because, nobody will want to update a cadastral map where there is a perceived change in vegetation/tree for instance. This leads to a decision stage where sunshades and vegetation classes are considered as the irrelevant classes and building extensions and mixed objects are considered as relevant classes. Sunshades and vegetation are obviously not relevant for updating the BAG map, because these classes, though remarkable changes, are not needed for the updating process. The building extensions are undisputable for map updates, but the mixed objects are equally considered as relevant because they may contain a variety of objects which often include building extensions.

As a consequence of these requirements, the error matrix table is then further classified into a matrix which contains relevant and irrelevant changes as seen below.

		Reference data		Total	Error of Commission	User Accuracy
		Relevant changes	Irrelevant Changes			
Classified data	Relevant	22	10	32	31	69
	Irrelevant	4	38	42	10	90
Total		26	48	74		
Error of Omission		15	21			
Producer accuracy		85	79			

Table 5-6: Error matrix for relevant and irrelevant classes.

This translates to 81% accuracy for identifying the relevant and irrelevant changes. With this, the relevant changes can be identified up to 69% accuracy and used for map updating. The 31% commission error implies that 31% of the changes flagged are regarded as false alarms, this will cause the operator to confirm those object during updating. For a large area this proportion might become cumbersome as many false alarms will need to be attended to but it is safer to confirm than omitting them. Having a 15% omission error for the relevant changes indicates that about 15% of the changes will not be identified; however it is important to note that the mixed objects class has a higher percentage in this omission which implies that detecting building extensions will not be greatly overlooked. Therefore only a few portions of the map may be left out-dated. By first filtering out the irrelevant changes which have a higher detection rate (90%) the focus on updating the relevant ones can be made easier. Conclusively, these results suggest that this classification is useful for obtaining desired results for updating maps.

In estimating the number of building contours that need updating, two scenarios have been considered. In the first scenario, a query has been executed to select all building contours that intersect objects in the relevant class. An offset of 0.5 is specified to cater for the shrinking of the polygons used to select points for classification. Out of 255 buildings, a count of 188 is attained. Taking a closer look at the results, it is observed that most selected changes are small area changes. It has been initially been stated that large

changes included objects whose bounding box length or width is more than 1m. In this case, all changes are considered, but when considering those strictly for map updating, another filter is considered to remove small area polygons from the relevant class. This leads to the second scenario where polygons less than 20m² are removed from the selection criteria; this threshold is chosen by considering the size of a remarkable extension to a building, which will be at least 20m². This idea is adopted from Teo and Shih (2013) who used a 50m² threshold to remove small areas in a nDSM. With the said threshold, a total of 93 out of 255 building contours are flagged for updating. This percentage is high and may not reflect the real situation. From further evaluation, it is observed that this outcome is affected by a couple of reasons. First, the already reported commission error which likely contributes 31 per cent of false alarms will increase the building count. Secondly, there are some instances where the change polygons extend to adjoining building contours, especially for the mixed classes; this causes a double count for the building contours thereby increasing the overall percentage needed for updating. See Figure 5-14 below.



Figure 5-14: Building polygons earmarked for updating (red) and those that are unchanged (black). The relevant changes are shown in the two classes of building extension (blue) and mixed objects (grey).

From Figure 5-14 above, it can already be seen by visual confirmation that some of the selected polygons for updating are selected as a result of the commission error. At the top left quarter of the figure, instances where multiple building contours are counted against one change polygon can be seen. This validates the fact that these effects can cause increased counts for building to be updated. The operator's discretion and intervention are may be required when dealing with these cases.

6. CONCLUSION AND RECOMMENDATIONS

6.1. Conclusion

This research was set up to meet several objectives. The accuracy of a 2D vector map is determined by comparing it with point cloud data from an ALS system. Comparisons are done by computing the point-to-line distances between the vertices from the point cloud building outline and the 2D map outline. But before that is implemented, the differences in the map are separated using a threshold which defines two sets of differences.

The threshold value is selected based on the minimum size of an object which passes for a real change. This results in two classes of differences –small and large differences. The small differences are used to determine the geometric accuracy of the map using the point-to-line distance and the large represent object change in the scene.

From the small differences, the accuracy of the 2D map dataset was found to be approximately 25cm which falls just short of the required accuracy of 20cm. The measure is tested for its robustness by independently splitting the area in to four blocks and all results are all within 10cm of the required accuracy. Given the underlying assumptions which modelled errors that are contributed by the point cloud data, it is reasonable to conclude that the map accuracy is a little less than required, even though there could be some outliers in the points used for computations, these effects are minimised by the great deal of sampling points from the point cloud vertices.

The large differences were interpreted by using a supervised classification scheme, where training samples were used to define rules for describing predefined classes –sunshades, buildings extensions, vegetation and mixed objects. The computations are based solely on the height information of the point cloud data. Classification results reached an overall accuracy of 70% with this approach. These changes are further classified into relevant and irrelevant changes to identify objects that are suitable for map updating.

In conclusion, all objectives were met and the map accuracies and classification results are presented.

6.2. Recommendations

For geometric accuracy determination, this approach can be expanded to 3D by possibly incorporating point-to-plane distance analysis to determine accuracy of building representations in three dimensions. This can find its applications in assessing the quality of 3D building models where the deviations are considered not only for the roof outlines, but also for wall faces and other building sides. Accuracy reports can be improved by including more measures that may portray map regions based on the magnitude of error distribution. For example, using a deviation map to visualise the magnitude of errors in the various parts of the map as used by Anil et al. (2013) for analysing the differences between a building model and point cloud data.

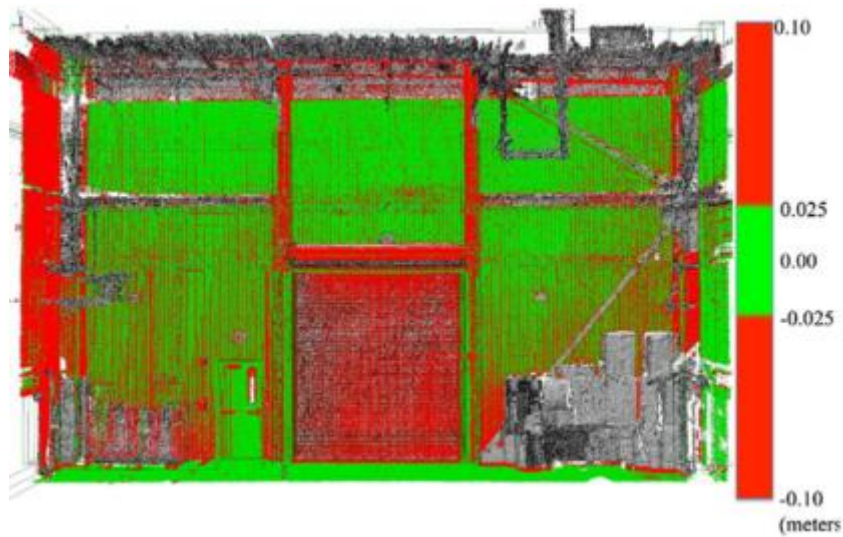


Figure 6-1: Example of a deviation map showing spread of error magnitude. Source: Anil et al. (2013).

The results of classification from the height attribute can also be improved by considering an integration of plane detection by segmentation to the histogram analysis. The segmentation properties for each of the classes can be different, for instance, building extensions and sunshades will have fewer planes while vegetation will likely have a high amount of planar segments. The segments can be analysed by considering their size, proximity to ground, roughness, spread etc. Semantic data may also be included to describe certain characteristics of the data, for example, if the structure contains walls all round, then it cannot be classified as sunshade. This kind of information can improve classification.

LIST OF REFERENCES

- Anil, E. B., Tang, P., Akinci, B., & Huber, D. (2013). Deviation Analysis Method for the Assessment of the Quality of the as-is Building Information Models Generated from Point Cloud Data. *Automation in Construction*, *35*, 507–516. doi:10.1016/j.autcon.2013.06.003
- Choi, K., Lee, I., & Kim, S. (2009). A Feature Based Approach to Automatic Change Detection from Lidar Data in Urban Areas. *International Archives of Photogrammetry and Remote Sensing* ., *XXXVIII*, 259–264.
- Ellenkamp, Y., & Maessen, B. (2009). Napoleon ’ s Registration Principles in Present Times : The Dutch System of Key Registers. In *Paper presented at the 11th International Conference for Spatial Data Infrastructure. The Netherlands. June 15-19,2009* (p. 15). Retrieved from <http://www.gsd.org/gsdiconf/gsd11/papers/pdf/101.pdf>
- Freire, S., Santos, T., Navarro, A., Soares, F., Silva, J. D., Afonso, N., ... Tenedório, J. (2014). Introducing Mapping Standards in the Quality Assessment of Buildings Extracted from Very High Resolution Satellite Imagery. *ISPRS Journal of Photogrammetry and Remote Sensing*, *90*, 1–9. doi:10.1016/j.isprsjprs.2013.12.009
- Gong, J., Sui, H., Ma, G., & Zhou, Q. (2008). A Review of Multi-Temporal Remote Sensing Data Change Detection. *The International Archives of the Photogrammetry, Remote Sensing and Spatial Information Sciences*, *XXXVII*, 757–762.
- Hebel, M., Arens, M., & Stilla, U. (2013). Change Detection in Urban Areas by Object-based Analysis and On-the-fly Comparison of Multi-view ALS Data. *ISPRS Journal of Photogrammetry and Remote Sensing*, *86*, 52–64. doi:10.1016/j.isprsjprs.2013.09.005
- Khoshelham, K., Nardinocchi, C., Frontoni, E., Mancini, A., & Zingaretti, P. (2010). Performance Evaluation of Automated Approaches to Building Detection in Multi-Source Aerial Data. *ISPRS Journal of Photogrammetry and Remote Sensing*, *65*(1), 123–133. doi:10.1016/j.isprsjprs.2009.09.005
- Malpica, J. A., Alonso, M. C., Papí, F., Arozarena, A., & Martínez De Agirre, A. (2013). Change Detection of Buildings from Satellite Imagery and Lidar Data. *International Journal of Remote Sensing*, *34*(5), 1652–1675. doi:10.1080/01431161.2012.725483
- Matikainen, L., Hyypä, J., Ahokas, E., Markelin, L., & Kaartinen, H. (2010). Automatic Detection of Buildings and Changes in Buildings for Updating of Maps. *Remote Sensing*, *2*(5), 1217–1248. doi:10.3390/rs2051217
- Murakami, H., Nakagawa, K., Hasegawa, H., Shibata, T., & Iwanami, E. (1999). Change Detection of Buildings Using an Airborne Laser Scanner. *ISPRS Journal of Photogrammetry and Remote Sensing*, *54*, 148–152.
- Oude Elberink, S., & Vosselman, G. (2011). Quality Analysis on 3D Building Models Reconstructed from Airborne Laser Scanning Data. *ISPRS Journal of Photogrammetry and Remote Sensing*, *66*(2), 157–165. doi:10.1016/j.isprsjprs.2010.09.009

- Rentsch, M., & Krzystek, P. (2009). Automatic Reconstructed Roof Shapes for Lidar Strip Adjustment and Quality Control. *International Archives of Photogrammetry and Remote Sensing*, XXXVIII, 2–7.
- Rutzinger, M., Ruf, B., Hofle, B., & Vetter, M. (2010). Change Detection of Building Footprints from Airborne Laser Scanning Acquired in Short Time Intervals. *ISPRS Annals of Photogrammetry, Remote Sensing and Spatial Information Sciences*, XXXVIII(1999), 475–480.
- Shannon, C. E. (1948). A Mathematical Theory of Communication. *The Bell System Technical Journal*, 27(July 1928), 379–423. doi:10.1145/584091.584093
- Singh, A. (1989). Review Article Digital Change Detection Techniques using Remotely-sensed Data. *International Journal of Remote Sensing*, 10(January 2015), 989–1003. doi:10.1080/01431168908903939
- Teo, T.-A., & Shih, T.-Y. (2013). Lidar-based Change Detection and Change-type Determination in Urban Areas. *International Journal of Remote Sensing*, 34(3), 968–981. doi:10.1080/01431161.2012.714504
- Van Coillie, F. M. B., Pires, R. L. V. P., Van Camp, N. A. F., & Gautama, S. (2008). Quantitative Segmentation Evaluation for Large Scale Mapping. In T. Blaschke, S. Lang, & G. J. Hay (Eds.), *Object-based image analysis-spatial concepts for knowledge-driven remote sensing applications*. (pp. 237–256). Springer-Verlag.
- Van der Sande, C., Soudarissanane, S., & Khoshelham, K. (2010). Assessment of Relative Accuracy of AHN-2 Laser Scanning Data Using Planar Features. *Sensors*, 10, 8198–8214. doi:10.3390/s100908198
- Vosselman, G. (2008). Analysis of Planimetric Accuracy of Airborne Laser Scanning Surveys. *International Archives of Photogrammetry and Remote Sensing, Commission(WG 3)*, 99–104.
- Vosselman, G. (2012). Automated Planimetric Quality Control in High Accuracy Airborne Laser Scanning Surveys. *ISPRS Journal of Photogrammetry and Remote Sensing*, 74, 90–100. doi:10.1016/j.isprsjprs.2012.09.002
- Vosselman, G., Sithole, G., & Gorte, B. G. H. (2004). Change Detection for Updating Medium Scale Maps Using Laser Altimetry. *The International Archives of the Photogrammetry, Remote Sensing and Spatial Information Sciences*, 34(Part B3), 6.
- Wikipedia. (2014). Delaunay Triangulation. Retrieved December 28, 2014, from http://en.wikipedia.org/wiki/Delaunay_triangulation
- Xu, S., Vosselman, G., & Oude Elberink, S. (2013). Detection and Classification of Changes in Buildings from Airborne Laser Scanning Data. *ISPRS Annals of Photogrammetry, Remote Sensing and Spatial Information Sciences*, II-5/W2(November), 343–348. doi:10.5194/isprsannals-II-5-W2-343-2013
- Xu, S., Vosselman, G., & Oude Elberink, S. (2014). Multiple-entity Based Classification of Airborne Laser Scanning Data in Urban Areas. *ISPRS Journal of Photogrammetry and Remote Sensing*, 88, 1–15. doi:10.1016/j.isprsjprs.2013.11.008

